

# Cross-comparison of Protein Recognition of Sialic Acid Diversity on Two Novel Sialoglycan Microarrays\*<sup>§</sup>

Received for publication, March 6, 2012, and in revised form, April 23, 2012. Published, JBC Papers in Press, May 1, 2012, DOI 10.1074/jbc.M112.359323

Vered Padler-Karavani<sup>†1</sup>, Xuezheng Song<sup>§1</sup>, Hai Yu<sup>¶</sup>, Nancy Hurtado-Ziola<sup>||</sup>, Shengshu Huang<sup>¶</sup>, Saddam Muthana<sup>¶</sup>, Harshal A. Chokhawala<sup>¶</sup>, Jiansong Cheng<sup>¶</sup>, Andrea Verhagen<sup>‡</sup>, Martijn A. Langereis<sup>\*\*</sup>, Ralf Kleene<sup>‡‡</sup>, Melitta Schachner<sup>§§</sup>, Raoul J. de Groot<sup>\*\*</sup>, Yi Lasanajak<sup>§</sup>, Haruo Matsuda<sup>¶¶</sup>, Richard Schwab<sup>‡</sup>, Xi Chen<sup>¶</sup>, David F. Smith<sup>§</sup>, Richard D. Cummings<sup>§2</sup>, and Ajit Varki<sup>‡3</sup>

From the <sup>†</sup>Department of Medicine and Cellular and Molecular Medicine, University of California, San Diego, La Jolla, California 92093, the <sup>§</sup>Department of Biochemistry, Glycomics Center, Emory University School of Medicine, Atlanta, Georgia 30322, the <sup>¶</sup>Department of Chemistry, University of California, Davis, California 95616, <sup>||</sup>Sialix, Inc., Vista, California 92081, the <sup>\*\*</sup>Virology Division, Department of Infectious Diseases and Immunology, Faculty of Veterinary Medicine, Utrecht University, Utrecht, The Netherlands, the <sup>‡‡</sup>Zentrum für Molekulare Neurobiologie, Universitätsklinikum Hamburg-Eppendorf, 20246 Hamburg, Germany, the <sup>§§</sup>Department of Biomedical Engineering, Rutgers University, Piscataway, New Jersey 08854, and the <sup>¶¶</sup>Department of Molecular and Applied Bioscience, Graduate School of Biosphere Science, Hiroshima University, Hiroshima 739-8528, Japan

**Background:** Various glycan microarrays are currently widely used, but systematic cross-comparisons are lacking.

**Results:** We compare and contrast two sialoglycan microarrays using a variety of sialic acid-binding proteins.

**Conclusion:** Diverse array formats can strengthen the quality of information, but differences between arrays may be observed.

**Significance:** Glycan arrays with similar glycan structures cannot be simply assumed to give similar results.

DNA and protein arrays are commonly accepted as powerful exploratory tools in research. This has mainly been achieved by the establishment of proper guidelines for quality control, allowing cross-comparison between different array platforms. As a natural extension, glycan microarrays were subsequently developed, and recent advances using such arrays have greatly enhanced our understanding of protein-glycan recognition in nature. However, although it is assumed that biologically significant protein-glycan binding is robustly detected by glycan microarrays, there are wide variations in the methods used to produce, present, couple, and detect glycans, and systematic cross-comparisons are lacking. We address these issues by comparing two arrays that together represent the marked diversity of sialic acid modifications, linkages, and underlying glycans in nature, including some identical motifs. We compare and contrast binding interactions with various known and novel plant, vertebrate, and viral sialic acid-recognizing proteins and present a technical advance for assessing specificity using mild periodate oxidation of the sialic acid chain. These data demonstrate both the diversity of sialic acids and the analytical power

of glycan arrays, showing that different presentations in different formats provide useful and complementary interpretations of glycan-binding protein specificity. They also highlight important challenges and questions for the future of glycan array technology and suggest that glycan arrays with similar glycan structures cannot be simply assumed to give similar results.

The advent of microarray technology has revolutionized biomedical research, shifting from single-molecule analysis to a system-wide high-throughput approach (1, 2). Both DNA and protein microarrays have since become established as powerful methods for genome and proteome investigations, respectively. They have been used for multiple applications, including expression profiling and identification of potential drug targets (3, 4). More recently, glycan microarray technology has also been developed for the high-throughput analysis of glycan-binding proteins (5–9).

Glycans cover the surface of all living cells in nature and participate in numerous biologically significant recognition events involving cells, bacteria, viruses, toxins, antibodies, lectins, and other glycan-binding proteins (GBPs)<sup>4</sup> (10). Glycan microarrays have been successfully used to characterize such glycan binding phenomena, thereby providing major insights into their specificity and underlying biological roles (5–7, 11–14). Such arrays were also used as platforms for biomarker discovery (15–17). Data from various glycan arrays are cur-

\* This work was supported, in whole or in part, by National Institutes of Health Grants R01GM32373 and U01 CA128442 (to A. V.), R01GM085448 (to D. F. S.), and R01GM076360 (to X. C.) and a bridging grant from the Consortium for Functional Glycomics under National Institutes of Health, NIGMS, Grant GM62116 (to R. D. C.). This work was also supported by an International Sepharadic Education Foundation postdoctoral fellowship (to V. P.-K.) and Defense Advanced Research Projects Agency Grant HR0011-10-00 (to R. D. C.). A. Varki is a cofounder of Sialix, Inc. (formerly Gc-Free, Inc.). N. Hurtado-Ziola is currently an employee of Sialix, Inc.

<sup>§</sup> This article contains supplemental Table 1 and Figs. 1–3.

<sup>1</sup> The contributions of the first two authors are equal.

<sup>2</sup> To whom correspondence may be addressed: Emory University School of Medicine, Atlanta, GA 30322. Tel.: 404-727-5962; Fax: 404-727-2738; E-mail: rdcummi@emory.edu.

<sup>3</sup> To whom correspondence may be addressed: University of California, San Diego, 9500 Gilman Dr., La Jolla, CA 92093-0687. Tel.: 858-534-2214; Fax: 858-534-5611; E-mail: a1varki@ucsd.edu.

<sup>4</sup> The abbreviations used are: NHS, *N*-hydroxysuccinimide; GBP, glycan-binding protein; Sia, sialic acid; Neu, neuraminic acid; Kdn, 2-keto-3-deoxynonulosonic acid; Neu5Ac, *N*-acetylneuraminic acid; Neu5Gc, *N*-glycolylneuraminic acid; LNnT, lacto-*N*-neo-tetraose; LNT, lacto-*N*-tetraose; NA2, asialo, galactosylated biantennary glycan; SNA, *S. nigra* agglutinin; Mal-1 and Mal-2, *M. amurensis* I and II, respectively; RFU, relative fluorescence units; BCoV, bovine coronavirus; BisTris, 2-[bis(2-hydroxyethyl)amino]-2-(hydroxymethyl)propane-1,3-diol.

## Cross-comparison of Two Sialoglycan Microarrays

rently accessible through databases such as that of the Consortium for Functional Glycomics (5, 6). However, it is currently unknown whether data from different array platforms with identical or similar glycan motifs can be directly compared.

In the early days of DNA microarrays, cross-comparison of different platforms posed the greatest challenge after the technique had been established. This eventually led to development of the Food and Drug Administration-initiated Microarray Quality Control Consortium (18) and the guidelines for the minimal information for microarray experiments (MIAME) (19). Given the markedly different structural and biophysical properties of glycans over nucleic acids and proteins, it is also likely to be challenging to compare glycan array data. Currently, there are several glycan array platforms, conjugation techniques, and linker groups, each encompassing unique groups of glycans (*e.g.* mammalian *versus* bacterial glycans) (5, 6, 8, 9). These differences make it currently difficult to cross-compare available glycan array data. On the other hand, comparisons of arrays that are focused on one major class of glycans are likely to generate interpretable information (*e.g.* arrays that contain terminal sialic acids as the common motif together with a wide collection of sialic acid binding modules that would ensure coverage of the various possible binding characteristics such as proteins, lectins, and viruses).

Sialic acids (Sias) are a large family (~50) of structurally unique and negatively charged nine-carbon backbone  $\alpha$ -ketoaldonic acids normally found at the terminal positions of various glycan chains on the cell surface of vertebrates or some pathogenic bacteria (20–22). All Sias are derivatives of neuraminic acid (Neu) or 2-keto-3-deoxynulosonic acid (Kdn), which contains a hydroxyl group instead of an *N*-acetyl group at C-5 position (20, 21). These can be further diversified by various modifications at the C-5 position (with acetyl or glycolyl) or the non-glycosidic hydroxyl groups (*e.g.* lactyl or phosphoryl may occur at the C-9 position, and methyl or sulfate groups may occur at the C-8 position) of Neu or the non-glycosidic hydroxyl groups in Kdn and can also be found as unsaturated, anhydro, or lactone forms (20, 21). The three most common Sias in mammals are *N*-acetylneuraminic acid (Neu5Ac), its hydroxylated form *N*-glycolylneuraminic acid (Neu5Gc), and the less abundant Kdn (20, 21). Recent advances in the methods for synthesizing various sialo-glycoconjugates (22–32) allowed collection of a large library of such glycans that was utilized to generate two extensive Sia-defined glycan microarrays (11, 15), which are valuable tools for identification and characterization of sialic acid-binding proteins and various lectins.

We report here the first ever direct cross-comparison of glycan recognition on two similar but unique glycan microarrays printed with glycans that share a terminal sialic acid. Together, they encompass one of the largest sialoglycan collections available to date and exemplify the diversity in Sia modifications, linkages, and underlying glycans. These arrays share some identical glycan motifs but use different platforms for glycan immobilization. The two arrays were reciprocally tested and analyzed in two laboratories with various Sia-binding proteins and viruses. These were tested at a wide range of concentrations while using several printers, buffer conditions, detection anti-

bodies, and scanners, and the data were compared side by side. Our findings demonstrate both the diversity in sialic acid recognition and the enhanced analytical power of comparing arrays as well as identifying challenges in comparisons of glycan microarray data and issues to address in future development of glycan microarray technology.

## EXPERIMENTAL PROCEDURES

**Sialoglycan Microarray Fabrication**—Array 1 was printed on epoxide-derivatized slides (Corning by Thermo Fisher Scientific) as described (15) with each glycoconjugate at 100  $\mu$ M in an optimized print buffer (300 mM phosphate buffer, pH 8.4) and as further detailed in the supplemental material. Array 2 was printed as described (11).

**Array Binding Assays**—Slides (Arrays 1 and 2) were incubated for 1 h in a staining dish with 50 °C prewarmed blocking solution (0.05 M ethanolamine in 0.1 M Tris, pH 9.0) to block the remaining reactive groups on the slide surface and then washed twice with 50 °C prewarmed distilled H<sub>2</sub>O. Slides were centrifuged at 200  $\times$  *g* for 3 min. Slides were then fitted with a ProPlate™ multiarray slide module (Invitrogen) to divide into the subarrays and then blocked with 200  $\mu$ l/subarray of Buffer 1 (PBS/OVA; 1% (w/v) ovalbumin in PBS, pH 7.4) for 1 h at room temperature with gentle shaking. Next, the blocking solution was aspirated, and diluted primary samples were added to each slide (in PBS/OVA, 200  $\mu$ l/subarray) and allowed to incubate with gentle shaking for 2 h at room temperature. Slides were washed three times with PBST (PBS containing 0.1% Tween) and then with PBS for 10 min/wash with shaking. Bound antibodies were detected by incubating with 200  $\mu$ l/subarray of the relevant fluorescence-labeled secondary antibody diluted in PBS at room temperature for 1 h. Slides were washed three times with PBST (PBS, 0.1% Tween) and then with PBS for 10 min/wash, followed by removal from the ProPlate™ multiarray slide module and immediate dipping of the slide into a staining dish with distilled H<sub>2</sub>O for 10 min with shaking, followed by centrifugation at 200  $\times$  *g* for 3 min. Dry slides were vacuum-sealed and stored in the dark until scanning the following day. Alternatively, Buffer 2 (BisTris, pH 6, 1 mM Ca<sup>2+</sup>, 1 mM Mg<sup>2+</sup>, 150 mM NaCl) was used. For blocking or lectin binding, Buffer 2 was supplemented with 1% ovalbumin, and for washing, it was supplemented with 0.1% Tween.

**Antibodies and Lectins**—Antibodies/lectins were diluted as described in the related figure legends. The biotinylated lectins *Sambucus nigra* agglutinin (SNA) and *Maackia amurensis* I and II (MAL-1 and MAL-2) were from Vector Laboratories. Affinity-purified polyclonal chicken anti-Neu5Gc IgY (pChGc) was prepared as described (33). Monoclonal chicken anti-Neu5Gc IgYs (mChGc6-1 and mChGc2-7) (34) were used as diluted hybridoma supernatants. Human immunoglobulin Fc fusion proteins of the viral lectin bovine coronavirus (BCoV) H<sup>+</sup>E<sup>0</sup>-Fc (35), the mouse lectins L1 (36) and CHL1 (37), and human Siglec-9 (38) were prepared as described. Cy3-streptavidin, Cy3-goat anti-human IgG (H+L), and Cy3-AffiniPure donkey-anti-chicken IgY (IgG)(H+L) were from Jackson ImmunoResearch Laboratories. The Alexa Fluor 633-goat anti-human IgG was from Invitrogen.

**Periodate Treatment to Detect Sia-specific Binding**—Slides were rehydrated for 10 min at room temperature and then either periodate-treated or mock-treated. For periodate treatment, slides were incubated with gentle shaking for 20 min at 4 °C in the dark with 200  $\mu$ l/subarray of freshly prepared cold 2 mM sodium metaperiodate in PBS, pH 6.5. The reaction was stopped by the addition of 50  $\mu$ l of 100 mM sodium borohydride in PBS, pH 6.5 (final concentration of 20 mM), followed by a 10-min incubation at room temperature with gentle shaking (the borohydride inactivates the periodate). Concurrently, as a mock control, periodate and borohydride solutions were pre-mixed (4:1), and slides were incubated with 250  $\mu$ l/subarray side by side with the periodate-treated slides. To remove resulting borates, arrays were then washed three times (10 min each wash) with 50 mM sodium acetate, pH 5.5, containing 100 mM NaCl and three times with PBS, pH 7.4. Subsequently, arrays were processed further as described (see “Array Binding Assays”).

**Array Slide Processing**—Slide assays were tested at two laboratories, and then analysis was conducted to compare reproducibility between them. Processed slides were reciprocally scanned by both laboratories and compared. At laboratory 1 (Scanner 1), slides were scanned as described (15) at 10  $\mu$ m resolution with a Genepix 4000B microarray scanner (Molecular Devices Corp., Union City, CA) using 350 or 450 gains, as indicated. Image analysis was carried out with Genepix Pro 6.0 analysis software (Molecular Devices Corp.). Spots were defined as circular features with a variable radius as determined by the Genepix scanning software. Local background subtraction was performed. At laboratory 2 (Scanner 2), slides were scanned using a ProScan Array (PerkinElmer Life Sciences) equipped with multiple lasers, and data were processed using the manufacturer’s software as described (11).

## RESULTS AND DISCUSSION

**Similarities and Differences between Two Sialylglycan Microarrays**—Among all vertebrate monosaccharides, sialic acids show the greatest structural diversity, which can be recognized by a wide variety of GBPs. To display and test the vast diversity of sialic acid modifications, linkages and underlying glycans in nature, we synthesized a library of naturally occurring and a few unnatural sialosides using efficient chemoenzymatic approaches (22) and applied them toward generation of two defined sialoglycan arrays (11, 15). Here, we compare these two arrays (sialoglycans listed in Table 1 and Table 2), together comprising 147 glycoconjugates, including 137 sialosides generated by combinations of 16 different Sias with 14 unique underlying glycan skeletons (summarized in Table 3). Both sets of glycans were covalently linked to an activated glass slide surface through a primary amino group. The terminal Sias encompassed the three common forms (Neu5Ac, Neu5Gc, and Kdn) and some of their hydroxyl-substituted derivatives with *O*-acetyl (at position C-9, C-5, or C-5-glycolyl), *O*-methyl (at position C-9, C-8, C-7, C-5, or C-5-glycolyl), or *O*-lactyl groups (C-9) (Tables 1 and 2). Importantly, although these glycan arrays were designed and constructed in separate laboratories with different emphases and on different printed surfaces, the sialic acid derivatives and sialylation methodologies were from

one single laboratory (22–32), ensuring comparability in this key aspect of the arrays. Array 1 (Table 1) was designed to analyze the most common, naturally occurring sialic acids (Neu5Ac, Neu5Gc, and their 9-*O*-acetylated derivatives Neu5,9Ac<sub>2</sub> and Neu5Gc9Ac) attached to over 10 different underlying glycan skeletons commonly present in nature. In contrast, Array 2 (Table 2) was designed to focus more on the broad diversity of sialic acids, being composed of only four underlying glycan skeletons but presenting 16 different sialic acids. The glycans of Array 1 were individually synthesized, purified, and printed by contact printing on epoxide-activated glass slides (15). In contrast, glycans of Array 2 were synthesized using a combinatorial approach using three fluorescently derivatized glycans as precursors and combinations of mannose derivatives, pyruvate, and appropriate enzymes (11). These glycans were then purified from the individual reactions, structurally identified, and printed on NHS-activated glass slides (11). Another difference in the two glycan sets is that they differ both in the structures of the linkers and in the fact that the reducing end monosaccharide of Array 2 glycans is in an open chain form. In contrast, the reducing ends of the glycans of Array 1 were maintained in their naturally occurring ring form (diagram in Table 3). Thus, although analyses of GBPs on the two arrays focus on their interactions with the sialylated non-reducing ends of the glycans, they are also potentially subject to the other differences mentioned above. Supplemental Table 1 shows a comparison of the 48 glycans that share common terminal glycan structures between the two arrays with the four sialic acids making up Array 1, and the differences are ranked, based on the differences in their underlying glycan skeletons.

**Assay and Analysis of Slide Arrays**—We analyzed the binding patterns of several plant, vertebrate, and viral sialic acid-recognizing proteins to the sialoglycans on both arrays at several optimal concentrations, side by side in two different laboratories, with the buffers and conditions as optimized for Array 1. The data generated were then compared between the different arrays. Briefly, arrays were blocked to prevent nonspecific binding and then incubated with diluted GBPs (in Buffer 1: PBS with 1% ovalbumin) for 2 h at room temperature and then washed, and binding was detected by applying a fluorescently labeled secondary antibody. Slides were then scanned, and fluorescent signals were analyzed to generate spreadsheet data files. Each glycan probe was printed in four replicates, and the signals were averaged. Replicate data points were corrected for outliers according to predefined rules (if coefficient of variation (%CV) was greater than 20%, replicate spots that fell outside the range of the mean  $\pm$  one S.D. were discarded) (11). To allow direct comparison of the specificity determinations between the two arrays, the binding was ranked as percentage of maximal signal in each array assay, and the relative rankings were then averaged to obtain the average rank of each glycan (5, 11). The average rank of each GBP was then ordered according to relevant common features (*i.e.* Sia type, linkage, underlying glycan structure, etc.), and the summary data were presented in a heat map.

**Recognition of  $\alpha$ 2-6-Sialyl Linkage by SNA Lectin on Two Arrays**—We compared binding patterns of a well known plant lectin SNA to the sialoglycans, using buffers and conditions

# Cross-comparison of Two Sialoglycan Microarrays

**TABLE 1**

**Listing and characteristics of sialoglycans on Array 1**

The listed compounds were covalently linked to epoxide-activated glass slides through their primary amine group using a contact printer.

SIALYL DERIVATIVE ARRAY 1										
Glycan ID	Sialic acid #	Linker	Linkage to linker	Skeleton	Abbreviation	Structure	Sialic Acid			
							Type	#Sial/KDN	Linkage	Valency
1	Sia-05	O(CH <sub>2</sub> ) <sub>3</sub> NH <sub>2</sub>	β	LacNAc	βLacNAc-3Sia-05	Neu5,9Ac <sub>2</sub> -α3Galβ4GlcNAcβO(CH <sub>2</sub> ) <sub>3</sub> NH <sub>2</sub>	Neu5,9Ac <sub>2</sub>	1	α3	Mono
2	Sia-06	O(CH <sub>2</sub> ) <sub>3</sub> NH <sub>2</sub>	β	LacNAc	βLacNAc-3Sia-06	Neu5Gc9Acα3Galβ4GlcNAcβO(CH <sub>2</sub> ) <sub>3</sub> NH <sub>2</sub>	Neu5Gc9Ac	1	α3	Mono
3	Sia-05	O(CH <sub>2</sub> ) <sub>3</sub> NH <sub>2</sub>	β	LacNAc	βLacNAc-6Sia-05	Neu5,9Ac <sub>2</sub> -α6Galβ4GlcNAcβO(CH <sub>2</sub> ) <sub>3</sub> NH <sub>2</sub>	Neu5,9Ac <sub>2</sub>	1	α6	Mono
4	Sia-06	O(CH <sub>2</sub> ) <sub>3</sub> NH <sub>2</sub>	β	LacNAc	βLacNAc-6Sia-06	Neu5Gc9Acα6Galβ4GlcNAcβO(CH <sub>2</sub> ) <sub>3</sub> NH <sub>2</sub>	Neu5Gc9Ac	1	α6	Mono
5	Sia-01	O(CH <sub>2</sub> ) <sub>3</sub> NH <sub>2</sub>	α	GalNAc	αGalNAc-6Sia-01	Neu5,9Ac <sub>2</sub> -α6GalNAcαO(CH <sub>2</sub> ) <sub>3</sub> NH <sub>2</sub>	Neu5Ac	1	α6	Mono
6	Sia-03	O(CH <sub>2</sub> ) <sub>3</sub> NH <sub>2</sub>	α	GalNAc	αGalNAc-6Sia-03	Neu5Gc9Acα6GalNAcαO(CH <sub>2</sub> ) <sub>3</sub> NH <sub>2</sub>	Neu5Gc	1	α6	Mono
7	Sia-05	O(CH <sub>2</sub> ) <sub>3</sub> NH <sub>2</sub>	β	Type1	βType1-3Sia-05	Neu5,9Ac <sub>2</sub> -α3Galβ3GlcNAcβO(CH <sub>2</sub> ) <sub>3</sub> NH <sub>2</sub>	Neu5,9Ac <sub>2</sub>	1	α3	Mono
8	Sia-06	O(CH <sub>2</sub> ) <sub>3</sub> NH <sub>2</sub>	β	Type1	βType1-3Sia-06	Neu5Gc9Acα3Galβ3GlcNAcβO(CH <sub>2</sub> ) <sub>3</sub> NH <sub>2</sub>	Neu5Gc9Ac	1	α3	Mono
9	Sia-05	O(CH <sub>2</sub> ) <sub>3</sub> NH <sub>2</sub>	α	Core1	αCore1-3Sia-05	Neu5,9Ac <sub>2</sub> -α3Galβ3GalNAcαO(CH <sub>2</sub> ) <sub>3</sub> NH <sub>2</sub>	Neu5,9Ac <sub>2</sub>	1	α3	Mono
10	Sia-06	O(CH <sub>2</sub> ) <sub>3</sub> NH <sub>2</sub>	α	Core1	αCore1-3Sia-06	Neu5Gc9Acα3Galβ3GalNAcαO(CH <sub>2</sub> ) <sub>3</sub> NH <sub>2</sub>	Neu5Gc9Ac	1	α3	Mono
11	Sia-01	O(CH <sub>2</sub> ) <sub>3</sub> NH <sub>2</sub>	β	LacNAc	βLacNAc-3Sia-01	Neu5Acα3Galβ4GlcNAcβO(CH <sub>2</sub> ) <sub>3</sub> NH <sub>2</sub>	Neu5Ac	1	α3	Mono
12	Sia-03	O(CH <sub>2</sub> ) <sub>3</sub> NH <sub>2</sub>	β	LacNAc	βLacNAc-3Sia-03	Neu5Gcα3Galβ4GlcNAcβO(CH <sub>2</sub> ) <sub>3</sub> NH <sub>2</sub>	Neu5Gc	1	α3	Mono
13	Sia-01	O(CH <sub>2</sub> ) <sub>3</sub> NH <sub>2</sub>	β	Type1	βType1-3Sia-01	Neu5Acα3Galβ3GlcNAcβO(CH <sub>2</sub> ) <sub>3</sub> NH <sub>2</sub>	Neu5Ac	1	α3	Mono
14	Sia-03	O(CH <sub>2</sub> ) <sub>3</sub> NH <sub>2</sub>	β	Type1	βType1-3Sia-03	Neu5Gcα3Galβ3GlcNAcβO(CH <sub>2</sub> ) <sub>3</sub> NH <sub>2</sub>	Neu5Gc	1	α3	Mono
15	Sia-01	O(CH <sub>2</sub> ) <sub>3</sub> NH <sub>2</sub>	α	Core1	αCore1-3Sia-01	Neu5Acα3Galβ3GalNAcαO(CH <sub>2</sub> ) <sub>3</sub> NH <sub>2</sub>	Neu5Ac	1	α3	Mono
16	Sia-03	O(CH <sub>2</sub> ) <sub>3</sub> NH <sub>2</sub>	α	Core1	αCore1-3Sia-03	Neu5Gcα3Galβ3GalNAcαO(CH <sub>2</sub> ) <sub>3</sub> NH <sub>2</sub>	Neu5Gc	1	α3	Mono
17	Sia-01	O(CH <sub>2</sub> ) <sub>3</sub> NH <sub>2</sub>	β	LacNAc	βLacNAc-6Sia-01	Neu5Acα6Galβ4GlcNAcβO(CH <sub>2</sub> ) <sub>3</sub> NH <sub>2</sub>	Neu5Ac	1	α6	Mono
18	Sia-03	O(CH <sub>2</sub> ) <sub>3</sub> NH <sub>2</sub>	β	LacNAc	βLacNAc-6Sia-03	Neu5Gcα6Galβ4GlcNAcβO(CH <sub>2</sub> ) <sub>3</sub> NH <sub>2</sub>	Neu5Gc	1	α6	Mono
19	Sia-01	O(CH <sub>2</sub> ) <sub>3</sub> NH <sub>2</sub>	β	Lactose	βLac-6Sia-01	Neu5Acα6Galβ4GlcβO(CH <sub>2</sub> ) <sub>3</sub> NH <sub>2</sub>	Neu5Ac	1	α6	Mono
20	Sia-03	O(CH <sub>2</sub> ) <sub>3</sub> NH <sub>2</sub>	β	Lactose	βLac-6Sia-03	Neu5Gcα6Galβ4GlcβO(CH <sub>2</sub> ) <sub>3</sub> NH <sub>2</sub>	Neu5Gc	1	α6	Mono
21	Sia-01	O(CH <sub>2</sub> ) <sub>3</sub> NH <sub>2</sub>	β	Lactose	βLac-3Sia-01	Neu5Acα3Galβ4GlcβO(CH <sub>2</sub> ) <sub>3</sub> NH <sub>2</sub>	Neu5Ac	1	α3	Mono
22	Sia-03	O(CH <sub>2</sub> ) <sub>3</sub> NH <sub>2</sub>	β	Lactose	βLac-3Sia-03	Neu5Gcα3Galβ4GlcβO(CH <sub>2</sub> ) <sub>3</sub> NH <sub>2</sub>	Neu5Gc	1	α3	Mono
23	Sia-05	O(CH <sub>2</sub> ) <sub>3</sub> NH <sub>2</sub>	α	GalNAc	αGalNAc-6Sia-05	Neu5,9Ac <sub>2</sub> -α6GalNAcαO(CH <sub>2</sub> ) <sub>3</sub> NH <sub>2</sub>	Neu5,9Ac <sub>2</sub>	1	α6	Mono
24	Sia-06	O(CH <sub>2</sub> ) <sub>3</sub> NH <sub>2</sub>	α	GalNAc	αGalNAc-6Sia-06	Neu5Gc9Acα6GalNAcαO(CH <sub>2</sub> ) <sub>3</sub> NH <sub>2</sub>	Neu5Gc9Ac	1	α6	Mono
25	Sia-01	O(CH <sub>2</sub> ) <sub>3</sub> NH <sub>2</sub>	β	Galactose	βGal-3Sia-01	Neu5Acα3GalβO(CH <sub>2</sub> ) <sub>3</sub> NH <sub>2</sub>	Neu5Ac	1	α3	Mono
26	Sia-03	O(CH <sub>2</sub> ) <sub>3</sub> NH <sub>2</sub>	β	Galactose	βGal-3Sia-03	Neu5Gcα3GalβO(CH <sub>2</sub> ) <sub>3</sub> NH <sub>2</sub>	Neu5Gc	1	α3	Mono
27	Sia-01	O(CH <sub>2</sub> ) <sub>3</sub> NH <sub>2</sub>	β	Galactose	βGal-6Sia-01	Neu5Acα6GalβO(CH <sub>2</sub> ) <sub>3</sub> NH <sub>2</sub>	Neu5Ac	1	α6	Mono
28	Sia-03	O(CH <sub>2</sub> ) <sub>3</sub> NH <sub>2</sub>	β	Galactose	βGal-6Sia-03	Neu5Gcα6GalβO(CH <sub>2</sub> ) <sub>3</sub> NH <sub>2</sub>	Neu5Gc	1	α6	Mono
29	Sia-05	O(CH <sub>2</sub> ) <sub>3</sub> NH <sub>2</sub>	β	Galactose	βGal-3Sia-05	Neu5,9Ac <sub>2</sub> -α3GalβO(CH <sub>2</sub> ) <sub>3</sub> NH <sub>2</sub>	Neu5,9Ac <sub>2</sub>	1	α3	Mono
30	Sia-06	O(CH <sub>2</sub> ) <sub>3</sub> NH <sub>2</sub>	β	Galactose	βGal-3Sia-06	Neu5Gc9Acα3GalβO(CH <sub>2</sub> ) <sub>3</sub> NH <sub>2</sub>	Neu5Gc9Ac	1	α3	Mono
31	Sia-05	O(CH <sub>2</sub> ) <sub>3</sub> NH <sub>2</sub>	β	Galactose	βGal-6Sia-05	Neu5,9Ac <sub>2</sub> -α6GalβO(CH <sub>2</sub> ) <sub>3</sub> NH <sub>2</sub>	Neu5,9Ac <sub>2</sub>	1	α6	Mono
32	Sia-06	O(CH <sub>2</sub> ) <sub>3</sub> NH <sub>2</sub>	β	Galactose	βGal-6Sia-06	Neu5Gc9Acα6GalβO(CH <sub>2</sub> ) <sub>3</sub> NH <sub>2</sub>	Neu5Gc9Ac	1	α6	Mono
33	Sia-01	O(CH <sub>2</sub> ) <sub>3</sub> NH <sub>2</sub>	β	Core1	βCore1-3Sia-01	Neu5Acα3Galβ3GalNAcβO(CH <sub>2</sub> ) <sub>3</sub> NH <sub>2</sub>	Neu5Ac	1	α3	Mono
34	Sia-03	O(CH <sub>2</sub> ) <sub>3</sub> NH <sub>2</sub>	β	Core1	βCore1-3Sia-03	Neu5Gcα3Galβ3GalNAcβO(CH <sub>2</sub> ) <sub>3</sub> NH <sub>2</sub>	Neu5Gc	1	α3	Mono
35	Sia-05	O(CH <sub>2</sub> ) <sub>3</sub> NH <sub>2</sub>	β	Core1	βCore1-3Sia-05	Neu5,9Ac <sub>2</sub> -α3Galβ3GalNAcβO(CH <sub>2</sub> ) <sub>3</sub> NH <sub>2</sub>	Neu5,9Ac <sub>2</sub>	1	α3	Mono
36	Sia-06	O(CH <sub>2</sub> ) <sub>3</sub> NH <sub>2</sub>	β	Core1	βCore1-3Sia-06	Neu5Gc9Acα3Galβ3GalNAcβO(CH <sub>2</sub> ) <sub>3</sub> NH <sub>2</sub>	Neu5Gc9Ac	1	α3	Mono
37	Sia-05	O(CH <sub>2</sub> ) <sub>3</sub> NH <sub>2</sub>	β	Lactose	βLac-6Sia-05	Neu5,9Ac <sub>2</sub> -α6Galβ4GlcβO(CH <sub>2</sub> ) <sub>3</sub> NH <sub>2</sub>	Neu5,9Ac <sub>2</sub>	1	α6	Mono
38	Sia-06	O(CH <sub>2</sub> ) <sub>3</sub> NH <sub>2</sub>	β	Lactose	βLac-6Sia-06	Neu5Gc9Acα6Galβ4GlcβO(CH <sub>2</sub> ) <sub>3</sub> NH <sub>2</sub>	Neu5Gc9Ac	1	α6	Mono
39	Sia-05	O(CH <sub>2</sub> ) <sub>3</sub> NH <sub>2</sub>	β	Lactose	βLac-3Sia-05	Neu5,9Ac <sub>2</sub> -α3Galβ4GlcβO(CH <sub>2</sub> ) <sub>3</sub> NH <sub>2</sub>	Neu5,9Ac <sub>2</sub>	1	α3	Mono
40	Sia-06	O(CH <sub>2</sub> ) <sub>3</sub> NH <sub>2</sub>	β	Lactose	βLac-3Sia-06	Neu5Gc9Acα3Galβ4GlcβO(CH <sub>2</sub> ) <sub>3</sub> NH <sub>2</sub>	Neu5Gc9Ac	1	α3	Mono
41	Sia-01	O(CH <sub>2</sub> ) <sub>3</sub> NH <sub>2</sub>	β	Lactose	βLac-3Sia-01-8Sia-01	Neu5Acα8Neu5Acα3Galβ4GlcβO(CH <sub>2</sub> ) <sub>3</sub> NH <sub>2</sub>	Neu5Ac-Neu5Ac	2	α3-α8	Mono
42	Sia-01	O(CH <sub>2</sub> ) <sub>3</sub> NH <sub>2</sub>	β	Lactose	βLac-3Sia-01-(8Sia-01) <sub>2</sub>	Neu5Acα8Neu5Acα8Neu5Acα3Galβ4GlcβO(CH <sub>2</sub> ) <sub>3</sub> NH <sub>2</sub>	(Neu5Ac) <sub>3</sub>	3	α3-α8	Mono
43	N/A	O(CH <sub>2</sub> ) <sub>3</sub> NH <sub>2</sub>	β	Lactose	βLac	Galβ4GlcβO(CH <sub>2</sub> ) <sub>3</sub> NH <sub>2</sub>	N/A	0	N/A	Mono
44	N/A	O(CH <sub>2</sub> ) <sub>3</sub> NH <sub>2</sub>	β	Lactose	βLac	Galβ4GlcNAcβO(CH <sub>2</sub> ) <sub>3</sub> NH <sub>2</sub>	N/A	0	N/A	Mono
45	N/A	O(CH <sub>2</sub> ) <sub>3</sub> NH <sub>2</sub>	β	Lactose	βLac	GalNAcαO(CH <sub>2</sub> ) <sub>3</sub> NH <sub>2</sub>	N/A	0	N/A	Mono
46	N/A	O(CH <sub>2</sub> ) <sub>3</sub> NH <sub>2</sub>	α	GalNAc	αGalNAc	GalNAcαO(CH <sub>2</sub> ) <sub>3</sub> NH <sub>2</sub>	N/A	0	N/A	Mono
47	N/A	O(CH <sub>2</sub> ) <sub>3</sub> NH <sub>2</sub>	α	GalNAc	αGalNAc	GalNAcαO(CH <sub>2</sub> ) <sub>3</sub> NH <sub>2</sub>	N/A	0	N/A	Mono
48	N/A	O(CH <sub>2</sub> ) <sub>3</sub> NH <sub>2</sub>	β	Galactose	βGal	GalβO(CH <sub>2</sub> ) <sub>3</sub> NH <sub>2</sub>	N/A	0	N/A	Mono
49	N/A	O(CH <sub>2</sub> ) <sub>3</sub> NH <sub>2</sub>	β	Galactose	βGal	GalβO(CH <sub>2</sub> ) <sub>3</sub> NH <sub>2</sub>	N/A	0	N/A	Mono
50	N/A	O(CH <sub>2</sub> ) <sub>3</sub> NH <sub>2</sub>	β	Core1	βCore1	Galβ3GalNAcβO(CH <sub>2</sub> ) <sub>3</sub> NH <sub>2</sub>	N/A	0	N/A	Mono
51	N/A	O(CH <sub>2</sub> ) <sub>3</sub> NH <sub>2</sub>	β	Type1	βType1	Galβ3GlcNAcβO(CH <sub>2</sub> ) <sub>3</sub> NH <sub>2</sub>	N/A	0	N/A	Mono
52	N/A	O(CH <sub>2</sub> ) <sub>3</sub> NH <sub>2</sub>	β	6S-LacNAc	6S-LacNAc	Galβ4GlcNAc6SβO(CH <sub>2</sub> ) <sub>3</sub> NH <sub>2</sub>	N/A	0	N/A	Mono
53	N/A	O(CH <sub>2</sub> ) <sub>3</sub> NH <sub>2</sub>	β	Le <sup>a</sup>	βLe <sup>a</sup> -3Sia-01	Neu5Acα3Galβ4(Fuco3)GlcNAcβO(CH <sub>2</sub> ) <sub>3</sub> NH <sub>2</sub>	Neu5Ac	1	α3	Mono
54	Sia-01	O(CH <sub>2</sub> ) <sub>3</sub> NH <sub>2</sub>	β	Le <sup>a</sup>	βLe <sup>a</sup> -3Sia-01	Neu5Gcα3Galβ4(Fuco3)GlcNAcβO(CH <sub>2</sub> ) <sub>3</sub> NH <sub>2</sub>	Neu5Gc	1	α3	Mono
55	Sia-03	O(CH <sub>2</sub> ) <sub>3</sub> NH <sub>2</sub>	β	Le <sup>a</sup>	βLe <sup>a</sup> -3Sia-03	Neu5Acα3Galβ4(Fuco3)GlcNAc6SβO(CH <sub>2</sub> ) <sub>3</sub> NH <sub>2</sub>	Neu5Ac	1	α3	Mono
56	Sia-01	O(CH <sub>2</sub> ) <sub>3</sub> NH <sub>2</sub>	β	6S-Le <sup>a</sup>	6S-βLe <sup>a</sup> -3Sia-01	Neu5Gcα3Galβ4(Fuco3)GlcNAc6SβO(CH <sub>2</sub> ) <sub>3</sub> NH <sub>2</sub>	Neu5Gc	1	α3	Mono
57	Sia-03	O(CH <sub>2</sub> ) <sub>3</sub> NH <sub>2</sub>	β	6S-Le <sup>a</sup>	6S-βLe <sup>a</sup> -3Sia-03	Neu5Gcα3Galβ4(Fuco3)GlcNAc6SβO(CH <sub>2</sub> ) <sub>3</sub> NH <sub>2</sub>	Neu5Gc	1	α3	Mono
58	Sia-03	O(CH <sub>2</sub> ) <sub>3</sub> NH <sub>2</sub>	β	6S-Le <sup>a</sup>	6S-βLe <sup>a</sup> -3Sia-03	Neu5Gcα3Galβ4(Fuco3)GlcNAc6SβO(CH <sub>2</sub> ) <sub>3</sub> NH <sub>2</sub>	Neu5Gc	1	α3	Mono
59	N/A	O(CH <sub>2</sub> ) <sub>3</sub> NH <sub>2</sub>	β	LNT	βLNT	Galβ3GlcNAcβ3Galβ4GlcβO(CH <sub>2</sub> ) <sub>3</sub> NH <sub>2</sub>	N/A	0	N/A	Mono
60	Sia-01	O(CH <sub>2</sub> ) <sub>3</sub> NH <sub>2</sub>	β	LNT	βLNT-3Sia-01	Neu5Acα3Galβ3GlcNAcβ3Galβ4GlcβO(CH <sub>2</sub> ) <sub>3</sub> NH <sub>2</sub>	Neu5Ac	1	α3	Mono
61	Sia-03	O(CH <sub>2</sub> ) <sub>3</sub> NH <sub>2</sub>	β	LNT	βLNT-3Sia-03	Neu5Gcα3Galβ3GlcNAcβ3Galβ4GlcβO(CH <sub>2</sub> ) <sub>3</sub> NH <sub>2</sub>	Neu5Gc	1	α3	Mono
62	Sia-01	O(CH <sub>2</sub> ) <sub>3</sub> NH <sub>2</sub>	β	6S-LacNAc	6S-βLacNAc-3Sia-01	Neu5Acα3Galβ4GlcNAc6SβO(CH <sub>2</sub> ) <sub>3</sub> NH <sub>2</sub>	Neu5Ac	1	α3	Mono
63	Sia-03	O(CH <sub>2</sub> ) <sub>3</sub> NH <sub>2</sub>	β	6S-LacNAc	6S-βLacNAc-3Sia-03	Neu5Gcα3Galβ4GlcNAc6SβO(CH <sub>2</sub> ) <sub>3</sub> NH <sub>2</sub>	Neu5Gc	1	α3	Mono
64	Sia-01	O(CH <sub>2</sub> ) <sub>3</sub> NHCOCH <sub>2</sub> (OCH <sub>2</sub> ) <sub>3</sub> NH <sub>2</sub>	β	Lactose	βLac-3Sia-01-(8Sia-01) <sub>2</sub>	Neu5Acα8Neu5Acα3Galβ4GlcβO(CH <sub>2</sub> ) <sub>3</sub> NHCOCH <sub>2</sub> (OCH <sub>2</sub> ) <sub>3</sub> NH <sub>2</sub>	Neu5Ac-Neu5Ac	2	α3-α8	Mono
65	Sia-01	O(CH <sub>2</sub> ) <sub>3</sub> NHCOCH <sub>2</sub> (OCH <sub>2</sub> ) <sub>3</sub> NH <sub>2</sub>	β	Lactose	βLac-3Sia-01-(8Sia-01) <sub>2</sub>	Neu5Acα8Neu5Acα8Neu5Acα3Galβ4GlcβO(CH <sub>2</sub> ) <sub>3</sub> NHCOCH <sub>2</sub> (OCH <sub>2</sub> ) <sub>3</sub> NH <sub>2</sub>	(Neu5Ac) <sub>3</sub>	3	α3-α8	Mono
66	Sia-01	O(CH <sub>2</sub> ) <sub>3</sub> NH <sub>2</sub>	β	Lactose	βLac-(3Sia-01)-6Sia-01	Neu5Acα6(Neu5Acα3)Galβ4GlcβO(CH <sub>2</sub> ) <sub>3</sub> NH <sub>2</sub>	Neu5Ac-Neu5Ac	2	α3/α6	Mono
67	Sia-01-(Sia-03)	O(CH <sub>2</sub> ) <sub>3</sub> NH <sub>2</sub>	β	Lactose	βLac-(3Sia-01)-6Sia-01	Neu5Acα6(Neu5Acα3)Galβ4GlcβO(CH <sub>2</sub> ) <sub>3</sub> NH <sub>2</sub>	Neu5Ac-Neu5Gc	2	α3/α6	Mono
68	Sia-01-(Sia-04)	O(CH <sub>2</sub> ) <sub>3</sub> NH <sub>2</sub>	β	Lactose	βLac-(3Sia-04)-6Sia-01	Neu5Acα6(Kdnα3)Galβ4GlcβO(CH <sub>2</sub> ) <sub>3</sub> NH <sub>2</sub>	Neu5Ac-Kdn	2	α3/α6	Mono
69	Sia-03-(Sia-01)	O(CH <sub>2</sub> ) <sub>3</sub> NH <sub>2</sub>	β	Lactose	βLac-(3Sia-01)-8Sia-03	Neu5Gcα8Neu5Acα3Galβ4GlcβO(CH <sub>2</sub> ) <sub>3</sub> NH <sub>2</sub>	Neu5Gc-Neu5Ac	2	α3-α8	Mono
70	Sia-04-(Sia-01)	O(CH <sub>2</sub> ) <sub>3</sub> NH <sub>2</sub>	β	Lactose	βLac-(3Sia-01)-8Sia-04	Kdnα8Neu5Acα3Galβ4GlcβO(CH <sub>2</sub> ) <sub>3</sub> NH <sub>2</sub>	Neu5Gc-Neu5Ac	2	α3-α8	Mono
71	Sia-01-(Sia-04)	O(CH <sub>2</sub> ) <sub>3</sub> NH <sub>2</sub>	β	Lactose	βLac-(3Sia-04)-8Sia-01	Neu5Acα8Kdnα6Galβ4GlcβO(CH <sub>2</sub> ) <sub>3</sub> NH <sub>2</sub>	Neu5Ac-Kdn	2	α3-α8	Mono
72	Sia-01-(Sia-03)	O(CH <sub>2</sub> ) <sub>3</sub> NH <sub>2</sub>	β	Lactose	βLac-(3Sia-03)-8Sia-01	Neu5Acα8Neu5Gcα3Galβ4GlcβO(CH <sub>2</sub> ) <sub>3</sub> NH <sub>2</sub>	Neu5Ac-Neu5Gc	2	α3-α8	Mono
73	Sia-01-(Sia-03)	O(CH <sub>2</sub> ) <sub>3</sub> NH <sub>2</sub>	β	Lactose	βLac-(3Sia-03)-8Sia-01	Neu5Acα8Neu5Gcα6Galβ4GlcβO(CH <sub>2</sub> ) <sub>3</sub> NH <sub>2</sub>	Neu5Ac-Neu5Gc	2	α3-α8	Mono
500	M			hlgG	hlgG	Human IgG	N/A	0	N/A	N/A
M				SA	SA <sub>888</sub>	Streptavidin Alexa555	N/A	0	N/A	N/A

optimized for Array 1. Biotinylated SNA shows the expected Siaα2–6-specific recognition on both arrays (at the same lectin concentration of 20 μg/ml; Fig. 1a), with the binding to Array 2 being more prominent. Binding was influenced by the type of Sia as well as by the underlying glycan structure, especially for Array 1 sialoglycans (Fig. 1d), which were presented on 10 underlying structures compared with only four underlying structures on Array 2 (Table 3). On Array 1, SNA bound better to 9-O-acetylated-Sia compared with the unmodified Sia attached to the same underlying glycan structures (Fig. 1d; Sia-05, Sia-06 > Sia-01, Sia-03) and further showed preference for the disaccharide skeletons Siaα2–6LacNAc followed by Siaα2–6Lac, over the monosaccharide skeletons Siaα2–6Gal, with almost no binding to Siaα2–6GalNAc (Fig. 1d). This suggests that the preferred SNA binding motif is a sialylated trisaccharide (Siaα2–6LacNAc) that is further stabilized by the Sia O-acetyl modification at the 9-position as well as by the

N-acetyl group at the third sugar from the non-reducing end. SNA recognized a sialylated disaccharide to a lesser extent. However, an N-acetyl group at the reducing end second sugar reduced the binding (Siaα2–6Gal > Siaα2–6GalNAc). Comparable binding patterns were also observed when we used two different contact printers to generate Array 1 (supplemental Fig. 1a; R<sup>2</sup> = 0.99) or when the same slide was scanned and analyzed with two different scanners (supplemental Fig. 1b; R<sup>2</sup> = 0.92).

On Array 2, SNA shows a clear skeleton preference to Siaα2–6LNT or Siaα2–6NA2 over Siaα2–6Lac or Siaα2–6LNT (Fig. 1d). In contrast to Siaα2–6LNT or Siaα2–6NA2, the Siaα2–6Lac lacks an N-acetyl group on the third monosaccharide from the

TABLE 2

Listing and characteristics of sialoglycans on Array 2

The listed compounds were covalently linked to NHS-activated glass slides through their primary amine group using a non-contact printer. AEAB, bifunctional fluorescent tag 2-amino-(*N*-aminoethyl) benzamide.

SIALYL DERIVATIVE ARRAY 2								
Glycan ID	Sialic acid #	Skeleton	Abbreviation	Structure	Sialic acid			
					Type	Linkage	Valency	
1	Sia-01	LNT	LNT-6Sia-01	Neu5Acα6Galβ4GlcNAcβ3Galβ4Glcitol-AEAB	Neu5Ac	α6	Mono	
2	Sia-02	LNT	LNT-6Sia-02	Neu5Ac8Meα6Galβ4GlcNAcβ3Galβ4Glcitol-AEAB	Neu5Ac8Me	α6	Mono	
3	Sia-03	LNT	LNT-6Sia-03	Neu5Gcα3Galβ4GlcNAcβ3Galβ4Glcitol-AEAB	Neu5Gc	α6	Mono	
4	Sia-04	LNT	LNT-6Sia-04	Kdnα6Galβ4GlcNAcβ3Galβ4Glcitol-AEAB	Kdn	α6	Mono	
5	Sia-05	LNT	LNT-6Sia-05	Neu5,9Ac <sub>2</sub> α6Galβ4GlcNAcβ3Galβ4Glcitol-AEAB	Neu5,9Ac <sub>2</sub>	α6	Mono	
6	Sia-06	LNT	LNT-6Sia-06	Neu5Gc9Acα6Galβ4GlcNAcβ3Galβ4Glcitol-AEAB	Neu5Gc9Ac	α6	Mono	
7	Sia-07	LNT	LNT-6Sia-07	Kdn9Acα6Galβ4GlcNAcβ3Galβ4Glcitol-AEAB	Kdn9Ac	α6	Mono	
8	Sia-08	LNT	LNT-6Sia-08	Neu5Ac9Meα6Galβ4GlcNAcβ3Galβ4Glcitol-AEAB	Neu5Ac9Me	α6	Mono	
9	Sia-09	LNT	LNT-6Sia-09	Neu5GcOMeα6Galβ4GlcNAcβ3Galβ4Glcitol-AEAB	Neu5GcOMe	α6	Mono	
10	Sia-10	LNT	LNT-6Sia-10	Kdn9Meα6Galβ4GlcNAcβ3Galβ4Glcitol-AEAB	Kdn9Me	α6	Mono	
11	Sia-12	LNT	LNT-6Sia-12	Kdn7Meα6Galβ4GlcNAcβ3Galβ4Glcitol-AEAB	Kdn7Me	α6	Mono	
12	Sia-13	LNT	LNT-6Sia-13	Neu5Ac9Ltα6Galβ4GlcNAcβ3Galβ4Glcitol-AEAB	Neu5Ac9Lt	α6	Mono	
13	Sia-14	LNT	LNT-6Sia-14	Neu5GcOAcα6Galβ4GlcNAcβ3Galβ4Glcitol-AEAB	Neu5GcOAc	α6	Mono	
14	Sia-15	LNT	LNT-6Sia-15	Kdn5Acα6Galβ4GlcNAcβ3Galβ4Glcitol-AEAB	Kdn5Ac	α6	Mono	
15	Sia-16	LNT	LNT-6Sia-16	Kdn5,9Ac <sub>2</sub> α6Galβ4GlcNAcβ3Galβ4Glcitol-AEAB	Kdn5,9Ac <sub>2</sub>	α6	Mono	
16	Sia-01	LNT	LNT-3Sia-01	Neu5Acα3Galβ4GlcNAcβ3Galβ4Glcitol-AEAB	Neu5Ac	α3	Mono	
17	Sia-02	LNT	LNT-3Sia-02	Neu5Ac8Meα3Galβ4GlcNAcβ3Galβ4Glcitol-AEAB	Neu5Ac8Me	α3	Mono	
18	Sia-03	LNT	LNT-3Sia-03	Neu5Gcα3Galβ4GlcNAcβ3Galβ4Glcitol-AEAB	Neu5Gc	α3	Mono	
19	Sia-04	LNT	LNT-3Sia-04	Kdnα3Galβ4GlcNAcβ3Galβ4Glcitol-AEAB	Kdn	α3	Mono	
20	Sia-05	LNT	LNT-3Sia-05	Neu5,9Ac <sub>2</sub> α3Galβ4GlcNAcβ3Galβ4Glcitol-AEAB	Neu5,9Ac <sub>2</sub>	α3	Mono	
21	Sia-06	LNT	LNT-3Sia-06	Neu5Gc9Acα3Galβ4GlcNAcβ3Galβ4Glcitol-AEAB	Neu5Gc9Ac	α3	Mono	
22	Sia-07	LNT	LNT-3Sia-07	Kdn9Acα3Galβ4GlcNAcβ3Galβ4Glcitol-AEAB	Kdn9Ac	α3	Mono	
23	Sia-08	LNT	LNT-3Sia-08	Neu5Ac9Meα3Galβ4GlcNAcβ3Galβ4Glcitol-AEAB	Neu5Ac9Me	α3	Mono	
24	Sia-09	LNT	LNT-3Sia-09	Neu5GcOMeα3Galβ4GlcNAcβ3Galβ4Glcitol-AEAB	Neu5GcOMe	α3	Mono	
25	Sia-11	LNT	LNT-3Sia-11	Kdn5Meα3Galβ4GlcNAcβ3Galβ4Glcitol-AEAB	Kdn5Me	α3	Mono	
26	Sia-12	LNT	LNT-3Sia-12	Kdn7Meα3Galβ4GlcNAcβ3Galβ4Glcitol-AEAB	Kdn7Me	α3	Mono	
27	Sia-13	LNT	LNT-3Sia-13	Neu5Ac9Ltα3Galβ4GlcNAcβ3Galβ4Glcitol-AEAB	Neu5Ac9Lt	α3	Mono	
28	Sia-14	LNT	LNT-3Sia-14	Neu5GcOAcα3Galβ4GlcNAcβ3Galβ4Glcitol-AEAB	Neu5GcOAc	α3	Mono	
29	Sia-15	LNT	LNT-3Sia-15	Kdn5Acα3Galβ4GlcNAcβ3Galβ4Glcitol-AEAB	Kdn5Ac	α3	Mono	
30	Sia-16	LNT	LNT-3Sia-16	Kdn5,9Ac <sub>2</sub> α3Galβ4GlcNAcβ3Galβ4Glcitol-AEAB	Kdn5,9Ac <sub>2</sub>	α3	Mono	
31	Sia-01	Lactose	Lac-6Sia-01	Neu5Acα6Galβ4Glcitol-AEAB	Neu5Ac	α6	Mono	
32	Sia-03	Lactose	Lac-6Sia-03	Neu5Gcα6Galβ4Glcitol-AEAB	Neu5Gc	α6	Mono	
33	Sia-01	Lactose	Lac-3Sia-01	Neu5Acα3Galβ4Glcitol-AEAB	Neu5Ac	α3	Mono	
34	Sia-03	Lactose	Lac-3Sia-03	Neu5Gcα3Galβ4Glcitol-AEAB	Neu5Gc	α3	Mono	
35	Sia-01	NA2	NA2-6Sia-01	Neu5Acα6Galβ4GlcNAcβ2Manα3(Neu5Acα6Galβ4GlcNAcβ2Manα6)Manβ4GlcNAcβ4GlcNAcitol-AEAB	Neu5Ac	α6	Di	
36	Sia-02	NA2	NA2-6Sia-02	Neu5Ac8Meα6Galβ4GlcNAcβ2Manα3(Neu5Ac8Meα6Galβ4GlcNAcβ2Manα6)Manβ4GlcNAcβ4GlcNAcitol-AEAB	Neu5Ac8Me	α6	Di	
37	Sia-03	NA2	NA2-6Sia-03	Neu5Gcα6Galβ4GlcNAcβ2Manα3(Neu5Gcα6Galβ4GlcNAcβ2Manα6)Manβ4GlcNAcβ4GlcNAcitol-AEAB	Neu5Gc	α6	Di	
38	Sia-05	NA2	NA2-6Sia-05	Neu5,9Ac <sub>2</sub> α6Galβ4GlcNAcβ2Manα3(Neu5,9Ac <sub>2</sub> α6Galβ4GlcNAcβ2Manα6)Manβ4GlcNAcβ4GlcNAcitol-AEAB	Neu5,9Ac <sub>2</sub>	α6	Di	
39	Sia-06	NA2	NA2-6Sia-06	Neu5Gc9Acα6Galβ4GlcNAcβ2Manα3(Neu5Gc9Acα6Galβ4GlcNAcβ2Manα6)Manβ4GlcNAcβ4GlcNAcitol-AEAB	Neu5Gc9Ac	α6	Di	
40	Sia-08	NA2	NA2-6Sia-08	*Neu5Ac9Meα6Galβ4GlcNAcβ2Manα3(Galβ4GlcNAcβ2Manα6)Manβ4GlcNAcβ4GlcNAcitol-AEAB	Neu5Ac9Me	α6	Mono	
41	Sia-09	NA2	NA2-6Sia-09	Neu5GcOMeα6Galβ4GlcNAcβ2Manα3(Neu5GcOMeα6Galβ4GlcNAcβ2Manα6)Manβ4GlcNAcβ4GlcNAcitol-AEAB	Neu5GcOMe	α6	Di	
42	Sia-10	NA2	NA2-6Sia-10	*Kdn9Meα6Galβ4GlcNAcβ2Manα3(Galβ4GlcNAcβ2Manα6)Manβ4GlcNAcβ4GlcNAcitol-AEAB	Kdn9Me	α6	Mono	
43	Sia-11	NA2	NA2-6Sia-11	*Kdn5Meα6Galβ4GlcNAcβ2Manα3(Galβ4GlcNAcβ2Manα6)Manβ4GlcNAcβ4GlcNAcitol-AEAB	Kdn5Me	α6	Mono	
44	Sia-12	NA2	NA2-6Sia-12	*Kdn7Meα6Galβ4GlcNAcβ2Manα3(Galβ4GlcNAcβ2Manα6)Manβ4GlcNAcβ4GlcNAcitol-AEAB	Kdn7Me	α6	Mono	
45	Sia-13	NA2	NA2-6Sia-13	Neu5Ac9Ltα6Galβ4GlcNAcβ2Manα3(Neu5Ac9Ltα6Galβ4GlcNAcβ2Manα6)Manβ4GlcNAcβ4GlcNAcitol-AEAB	Neu5Ac9Lt	α6	Di	
46	Sia-14	NA2	NA2-6Sia-14	Neu5GcOAcα6Galβ4GlcNAcβ2Manα3(Neu5GcOAcα6Galβ4GlcNAcβ2Manα6)Manβ4GlcNAcβ4GlcNAcitol-AEAB	Neu5GcOAc	α6	Di	
47	Sia-15	NA2	NA2-6Sia-15	Kdn5Acα6Galβ4GlcNAcβ2Manα3(Kdn5Acα6Galβ4GlcNAcβ2Manα6)Manβ4GlcNAcβ4GlcNAcitol-AEAB	Kdn5Ac	α6	Di	
48	Sia-01	NA2	NA2-3Sia-01	Neu5Acα3Galβ4GlcNAcβ2Manα3(Neu5Acα6Galβ4GlcNAcβ2Manα6)Manβ4GlcNAcβ4GlcNAcitol-AEAB	Neu5Ac	α3	Mono	
49	Sia-02	NA2	NA2-3Sia-02	*Neu5Ac8Meα3Galβ4GlcNAcβ2Manα3(Galβ4GlcNAcβ2Manα6)Manβ4GlcNAcβ4GlcNAcitol-AEAB	Neu5Ac8Me	α3	Mono	
50	Sia-03	NA2	NA2-3Sia-03	Neu5Gcα3Galβ4GlcNAcβ2Manα3(Neu5Gcα6Galβ4GlcNAcβ2Manα6)Manβ4GlcNAcβ4GlcNAcitol-AEAB	Neu5Gc	α3	Mono	
51	Sia-04	NA2	NA2-3Sia-04	Kdnα3Galβ4GlcNAcβ2Manα3(Kdnα6Galβ4GlcNAcβ2Manα6)Manβ4GlcNAcβ4GlcNAcitol-AEAB	Kdn	α3	Di	
52	Sia-05	NA2	NA2-3Sia-05	*Neu5,9Ac <sub>2</sub> α3Galβ4GlcNAcβ2Manα3(Galβ4GlcNAcβ2Manα6)Manβ4GlcNAcβ4GlcNAcitol-AEAB	Neu5,9Ac <sub>2</sub>	α3	Mono	
53	Sia-06	NA2	NA2-3Sia-06	Neu5Gc9Acα3Galβ4GlcNAcβ2Manα3(Neu5Gc9Acα6Galβ4GlcNAcβ2Manα6)Manβ4GlcNAcβ4GlcNAcitol-AEAB	Neu5Gc9Ac	α3	Di	
54	Sia-07	NA2	NA2-3Sia-07	*Kdn9Acα3Galβ4GlcNAcβ2Manα3(Galβ4GlcNAcβ2Manα6)Manβ4GlcNAcβ4GlcNAcitol-AEAB	Kdn9Ac	α3	Mono	
55	Sia-08	NA2	NA2-3Sia-08	*Neu5Ac9Meα3Galβ4GlcNAcβ2Manα3(Galβ4GlcNAcβ2Manα6)Manβ4GlcNAcβ4GlcNAcitol-AEAB	Neu5Ac9Me	α3	Mono	
56	Sia-09	NA2	NA2-3Sia-09	Neu5GcOMeα3Galβ4GlcNAcβ2Manα3(Neu5GcOMeα6Galβ4GlcNAcβ2Manα6)Manβ4GlcNAcβ4GlcNAcitol-AEAB	Neu5GcOMe	α3	Di	
57	Sia-10	NA2	NA2-3Sia-10	*Kdn9Meα3Galβ4GlcNAcβ2Manα3(Galβ4GlcNAcβ2Manα6)Manβ4GlcNAcβ4GlcNAcitol-AEAB	Kdn9Me	α3	Mono	
58	Sia-11	NA2	NA2-3Sia-11	*Kdn5Meα3Galβ4GlcNAcβ2Manα3(Galβ4GlcNAcβ2Manα6)Manβ4GlcNAcβ4GlcNAcitol-AEAB	Kdn5Me	α3	Mono	
59	Sia-12	NA2	NA2-3Sia-12	*Kdn7Meα3Galβ4GlcNAcβ2Manα3(Galβ4GlcNAcβ2Manα6)Manβ4GlcNAcβ4GlcNAcitol-AEAB	Kdn7Me	α3	Mono	
60	Sia-13	NA2	NA2-3Sia-13	Neu5Ac9Ltα3Galβ4GlcNAcβ2Manα3(Neu5Ac9Ltα6Galβ4GlcNAcβ2Manα6)Manβ4GlcNAcβ4GlcNAcitol-AEAB	Neu5Ac9Lt	α3	Di	
61	Sia-14	NA2	NA2-3Sia-14	*Neu5GcOAcα3Galβ4GlcNAcβ2Manα3(Galβ4GlcNAcβ2Manα6)Manβ4GlcNAcβ4GlcNAcitol-AEAB	Neu5GcOAc	α3	Mono	
62	Sia-15	NA2	NA2-3Sia-15	Kdn5Acα3Galβ4GlcNAcβ2Manα3(Kdn5Acα6Galβ4GlcNAcβ2Manα6)Manβ4GlcNAcβ4GlcNAcitol-AEAB	Kdn5Ac	α3	Di	
63	Sia-01	LNT	LNT-3Sia-01	Neu5Acα3Galβ3GlcNAcβ3Galβ4Glcitol-AEAB	Neu5Ac	α3	Mono	
64	Sia-03	LNT	LNT-3Sia-03	Neu5Gcα3Galβ3GlcNAcβ3Galβ4Glcitol-AEAB	Neu5Gc	α3	Mono	
65	Sia-05	LNT	LNT-3Sia-05	Neu5,9Ac <sub>2</sub> α3Galβ3GlcNAcβ3Galβ4Glcitol-AEAB	Neu5,9Ac <sub>2</sub>	α3	Mono	
66	Sia-07	LNT	LNT-3Sia-07	Kdn9Acα3Galβ3GlcNAcβ3Galβ4Glcitol-AEAB	Kdn9Ac	α3	Mono	
67	Sia-09	LNT	LNT-3Sia-09	Neu5GcOMeα3Galβ3GlcNAcβ3Galβ4Glcitol-AEAB	Neu5GcOMe	α3	Mono	
68	Sia-01	LNT	LNT-6Sia-01	Neu5Acα6Galβ3GlcNAcβ3Galβ4Glcitol-AEAB	Neu5Ac	α6	Mono	
69	Sia-03	LNT	LNT-6Sia-03	Neu5Gcα6Galβ3GlcNAcβ3Galβ4Glcitol-AEAB	Neu5Gc	α6	Mono	
70	Sia-04	LNT	LNT-6Sia-04	Kdnα6Galβ3GlcNAcβ3Galβ4Glcitol-AEAB	Kdn	α6	Mono	
71	Sia-05	LNT	LNT-6Sia-05	Neu5,9Ac <sub>2</sub> α6Galβ3GlcNAcβ3Galβ4Glcitol-AEAB	Neu5,9Ac <sub>2</sub>	α6	Mono	
72	Sia-07	LNT	LNT-6Sia-07	Kdn9Acα6Galβ3GlcNAcβ3Galβ4Glcitol-AEAB	Kdn9Ac	α6	Mono	
73	Sia-09	LNT	LNT-6Sia-09	Neu5GcOMeα6Galβ3GlcNAcβ3Galβ4Glcitol-AEAB	Neu5GcOMe	α6	Mono	
74	Sia-11	LNT	LNT-6Sia-11	Kdn5Meα6Galβ3GlcNAcβ3Galβ4Glcitol-AEAB	Kdn5Me	α6	Mono	
75	Sia-13	LNT	LNT-6Sia-13	Neu5Ac9Ltα6Galβ3GlcNAcβ3Galβ4Glcitol-AEAB	Neu5Ac9Lt	α6	Mono	
76	Sia-14	LNT	LNT-6Sia-14	Neu5GcOAcα6Galβ3GlcNAcβ3Galβ4Glcitol-AEAB	Neu5GcOAc	α6	Mono	
77	Sia-15	LNT	LNT-6Sia-15	Kdn5Acα6Galβ3GlcNAcβ3Galβ4Glcitol-AEAB	Kdn5Ac	α6	Mono	
78	Sc	LNT	LNT	Galβ4GlcNAcβ3Galβ4Glcitol-AEAB	N/A	N/A	N/A	
79	Sc	NA2	NA2	Galβ4GlcNAcβ2Manα3(Neu5Acα6Galβ4GlcNAcβ2Manα6)Manβ4GlcNAcβ4GlcNAcitol-AEAB	N/A	N/A	N/A	
80	Sc	Man5	Man5	Manα6(Manα3)Manα6(Manα3)Manβ4GlcNAcβ4GlcNAcitol-AEAB	N/A	N/A	N/A	
81	N/A	PBS	PBS		N/A	N/A	N/A	
82	N/A	PBS	PBS		N/A	N/A	N/A	
83	N/A	PBS	PBS		N/A	N/A	N/A	
84	N/A	Biotin	Biotin		N/A	N/A	N/A	

Downloaded from www.jbc.org at Universiteitsbibliotheek Utrecht on November 9, 2012

## Cross-comparison of Two Sialoglycan Microarrays

**TABLE 3**

Combined summary of overall characteristics of glycoconjugates, sialosides, Sia types, underlying glycan skeletons, and linkers on the two sialoglycan arrays, including a diagram of glycans as found attached to each array surface

	Abbreviation	Underlying Skeleton Structure	Total Glycans with Skeleton	Sia-Glycans	Sialic acid #	Linker types	Sialic Acid Designations	
							Sialic acid #	Sialic Acid Types
<b>ARRAY 1:</b>								
1	Galactose	Gal	9	8	Sia-01, Sia-03, Sia-05, Sia-06	Linker-01	Sia-01	Neu5Ac
2	GalNAc	GalNAc	5	4	Sia-01, Sia-03, Sia-05, Sia-06	Linker-01	Sia-02	Neu5Ac8Me
3	Lactose	Gal $\beta$ 4Glc	21	20	Sia-01, Sia-03, Sia-04, Sia-05, Sia-06	Linker-01, Linker-02	Sia-03	Neu5Gc
4	LacNAc	Gal $\beta$ 4GlcNAc	9	8	Sia-01, Sia-03, Sia-05, Sia-06	Linker-01	Sia-04	Kdn
5	6S-LacNAc	Gal $\beta$ 4GlcNAc6S	3	2	Sia-01, Sia-03	Linker-01	Sia-05	Neu5,9Ac <sub>2</sub>
6	Type1	Gal $\beta$ 3GlcNAc	5	4	Sia-01, Sia-03, Sia-05, Sia-06	Linker-01	Sia-06	Neu5Gc9Ac
7	Core1	Gal $\beta$ 3GalNAc	9	8	Sia-01, Sia-03, Sia-05, Sia-06	Linker-01	Sia-07	Kdn9Ac
8	Le'	Gal $\beta$ 4(Fuca3)GlcNAc	2	2	Sia-01, Sia-03	Linker-01	Sia-08	Neu5Ac9Me
9	6S-Le'	Gal $\beta$ 4(Fuca3)GlcNAc6S	2	2	Sia-01, Sia-03	Linker-01	Sia-09	Neu5GcOMe
10	LNT	Gal $\beta$ 3GlcNAc $\beta$ 3Gal $\beta$ 4Glc	3	2	Sia-01, Sia-03	Linker-01	Sia-10	Kdn9Me
<b>Subtotal directly conjugated glycans on Array 1:</b>			<b>68</b>	<b>60</b>			Sia-11	Kdn5Me
<b>ARRAY 2:</b>								
1	NA2	Gal $\beta$ 4GlcNAc $\beta$ 2Man $\alpha$ 3(Gal $\beta$ 4GlcNAc $\beta$ 2Man $\alpha$ 6)Man $\beta$ 4GlcNAc $\beta$ 4GlcNAcitol	29	28	Sia-01, Sia-02, Sia-03, Sia-04, Sia-05, Sia-06, Sia-07, Sia-08, Sia-09, Sia-10, Sia-11, Sia-12, Sia-13, Sia-14, Sia-15	Linker-03	Sia-11	Kdn5Me
2	LNnT	Gal $\beta$ 4GlcNAc $\beta$ 3Gal $\beta$ 4Glcitol	31	30	Sia-01, Sia-02, Sia-03, Sia-04, Sia-05, Sia-06, Sia-07, Sia-08, Sia-09, Sia-10, Sia-11, Sia-12, Sia-13, Sia-14, Sia-15, Sia-16	Linker-03	Sia-12	Kdn7Me
3	LNT	Gal $\beta$ 3GlcNAc $\beta$ 3Gal $\beta$ 4Glcitol	15	15	Sia-01, Sia-03, Sia-04, Sia-05, Sia-07, Sia-09, Sia-11, Sia-13, Sia-14, Sia-15	Linker-03	Sia-13	Neu5Ac9Lt
4	Lactose	Gal $\beta$ 4Glcitol	4	4	Sia-01, Sia-03	Linker-03	Sia-14	Neu5GcOAc
<b>Subtotal directly conjugated glycans on Array 2:</b>			<b>79</b>	<b>77</b>			Sia-15	Kdn5Ac
<b>TOTAL GLYCANS ON TWO ARRAYS:</b>			<b>147</b>	<b>137</b>			Sia-16	Kdn5,9Ac <sub>2</sub>

**ARRAY 1**

Linker-01: O(CH<sub>2</sub>)<sub>2</sub>CH<sub>2</sub>NH<sub>2</sub>

Linker-02: O(CH<sub>2</sub>)<sub>3</sub>NHCOCH<sub>2</sub>(OCH<sub>2</sub>CH<sub>2</sub>)<sub>6</sub>NH<sub>2</sub>

**ARRAY 2**

Linker-03: N-(aminoethyl)-2-amino benzamide (AEAB)

**Sialic Acid Designations**

Sialic acid #	Sialic Acid Types
Sia-01	Neu5Ac
Sia-02	Neu5Ac8Me
Sia-03	Neu5Gc
Sia-04	Kdn
Sia-05	Neu5,9Ac <sub>2</sub>
Sia-06	Neu5Gc9Ac
Sia-07	Kdn9Ac
Sia-08	Neu5Ac9Me
Sia-09	Neu5GcOMe
Sia-10	Kdn9Me
Sia-11	Kdn5Me
Sia-12	Kdn7Me
Sia-13	Neu5Ac9Lt
Sia-14	Neu5GcOAc
Sia-15	Kdn5Ac
Sia-16	Kdn5,9Ac <sub>2</sub>

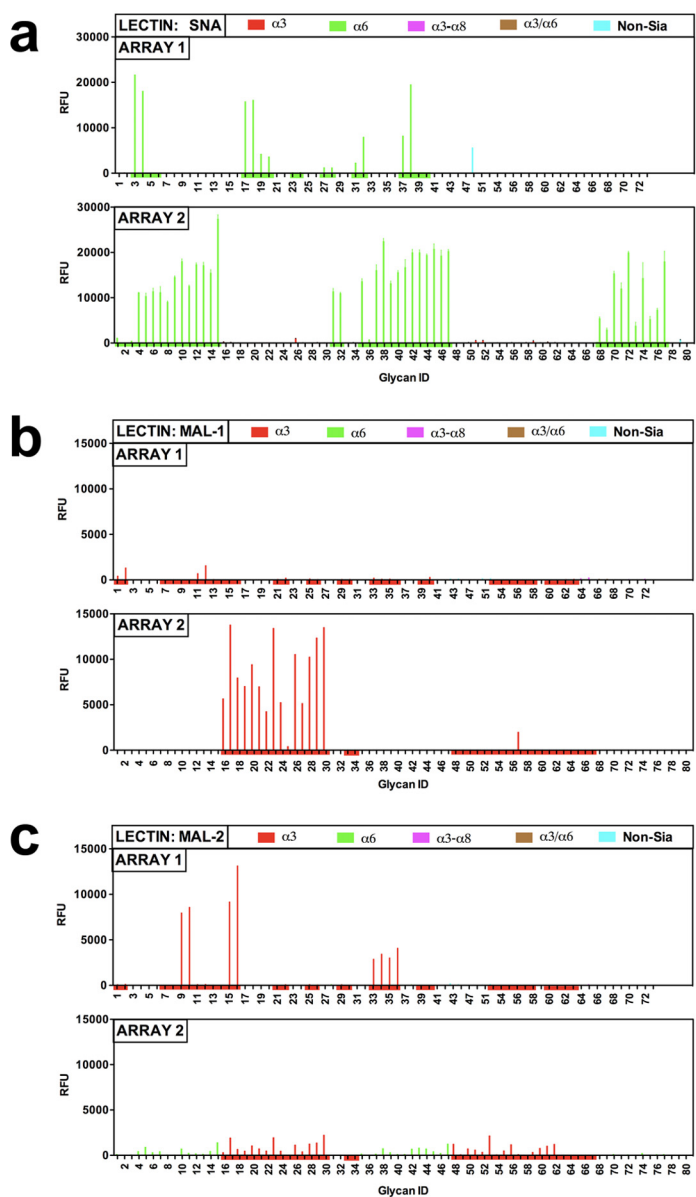
6LNnT/NA2 is probably due to the different linkages of the underlying galactosides (Sia $\alpha$ 2–6Gal $\beta$ 1–3GlcNAc $\beta$ -R in Sia $\alpha$ 2–6LNnT *versus* Sia $\alpha$ 2–6Gal $\beta$ 1–4GlcNAc $\beta$ -R in Sia $\alpha$ 2–6LNnT/NA2, respectively), indicating a preference toward the natural Sia $\alpha$ 2–6Gal $\beta$ 1–4 linkage over unnatural Sia $\alpha$ 2–6Gal $\beta$ 1–3 linkage to the third monosaccharide from the non-reducing end.

As with Array 1, modifications of the terminal Sia affect SNA binding to Array 2 sialoglycans, especially at positions 5, 8, and 9. On sialylated LNnT, acetyl groups at both the C-5 amino group and the C-9 hydroxyl group of sialic acid stabilize the binding (Fig. 1*d*; glycan 15 *versus* 7, 14, or 4 and glycan 5 *versus* 1 or 4), whereas a methyl modification at position 8 completely abolished binding (Fig. 1*d*; glycan 2). Furthermore, the type of modification at these positions greatly influenced the binding; whereas the acetyl group at position 9 added stability (*i.e.* glycan 5 with terminal Neu5,9Ac<sub>2</sub>), replacing it with the longer lactyl group (glycan 12, with terminal Neu5Ac9Lt) or with the smaller methyl group (glycan 8, with terminal Neu5Ac9Me) dramatically reduced the binding efficiency (glycans 5, 8, and 12 ranked 95, 62, and 55, respectively). The *N*-acetyl group at the 5-position was similarly optimal for binding (*i.e.* glycan 5) because replacing it with *N*-glycolyl (glycan 6), *N*-methylglycolyl (glycan 9), or *N*-acetylglycolyl (glycan 13) all reduced binding (glycans 5, 6, 9, and 13 ranked 95, 70, 59, and 68, respectively). SNA

binding pattern on Array 2 is similar to previous analysis conducted in different buffer conditions (11). Overall, despite differences in relative fluorescence units (RFU) values at comparable concentrations, the data from Array 1 and Array 2 complement each other and together provide a detailed view of the optimal recognition of sialylated glycans by SNA.

**Recognition of Sia $\alpha$ 2–3 Linkage by MAL-1 and MAL-2**—Both arrays were probed with plant lectins known to recognize the terminal Sia $\alpha$ 2–3 motif, MAL-1 and MAL-2 (also known as MAH). The biotinylated lectins showed different binding patterns on the two arrays; MAL-1 showed very low binding on Array 1 but showed strong binding to some Sia $\alpha$ 2–3-glycans on Array 2, whereas MAL-2 showed very low nonspecific binding on Array 2 but strong binding to Sia $\alpha$ 2–3-glycans on Array 1 (Fig. 1, *b* and *c*). Similar results were observed when the same slide was scanned and analyzed with two different scanners (supplemental Fig. 1*b*;  $R^2 = 0.92$ ).

On Array 1, MAL-1 bound to its known ligand (Sia $\alpha$ 2–3Gal $\beta$ 1–4GlcNAc; Fig. 1*d*) with much lower RFU values compared with Array 2 (at the same lectin concentration of 40  $\mu$ g/ml; see Fig. 1*b*), where many of the Sia $\alpha$ 2–3-glycans with underlying Type 2 glycans were bound (Array 2; Fig. 1*d*). Inspection of the ranked glycans on the two arrays indicated that on Array 1, MAL-1 shows very weak binding to Sia $\alpha$ 2–3-glycans but with specificity toward Sia $\alpha$ 2–3LacNAc (glycans



**d**

		LECTINS													
		ARRAY 1					ARRAY 2								
		Linkage		Rank		Linkage		Rank		Linkage					
Linkage	Skeleton	Sia #	Linkage to linker	MAL-1	MAL-2	SNA	Glycan ID	Linkage	Skeleton	Sia #	MAL-1	MAL-2	SNA	Glycan ID	Rank scale (Percentile)
α3	LNT	Type1	β	S-05	1	1	1	7	NA2	S-02	15	0	0	49	100 75 50 25 0
		S-06		0	1	1	8	S-05		5	1	52			
		S-03		1	1	0	14	S-07		7	0	54			
	6S-Le <sup>x</sup>	S-01	0	1	0	13	S-08	28	0	55					
		S-03	-1	1	0	61	S-10	9	33	57					
		S-01	5	0	0	60	S-11	33	0	58					
	Lac	S-03	1	0	0	38	S-12	18	2	59					
		S-01	6	0	0	57	S-14	9	1	61					
		S-03	2	1	0	56	S-01	0	54	63					
	LacNAc	S-01	2	0	0	55	S-03	1	57	64					
		S-05	6	1	1	39	S-05	1	9	65					
		S-03	5	1	1	22	S-07	1	37	66					
	Gal	S-01	5	1	0	21	S-09	1	25	67					
		S-06	19	1	0	40	S-01	23	16	2	16				
		S-05	30	1	1	1	S-02	72	83	1	17				
Core1	S-01	31	1	0	11	S-03	35	34	0	18					
	S-03	100	2	0	12	S-04	28	22	0	19					
	S-06	-1	1	1	30	S-05	46	42	0	20					
α	S-05	7	1	1	29	S-06	34	33	0	21					
	S-01	4	1	1	25	S-07	25	23	0	22					
	S-03	8	1	0	26	S-08	80	87	0	23					
β	S-01	16	5	1	33	S-09	26	22	0	24					
	S-03	1	6	0	34	S-11	3	4	0	25					
	S-05	-1	10	1	35	S-12	62	52	5	26					
α	S-06	2	38	1	36	S-13	21	20	0	27					
	S-01	3	67	0	15	S-14	51	55	0	28					
	S-03	4	100	0	16	S-15	70	56	0	29					
β	S-05	0	66	1	9	S-16	85	100	0	30					
	S-06	19	36	1	10	S-01	1	1	0	33					
	S-01	16	1	1	62	S-03	0	3	0	34					
α3-α8	Lac	S-01	6	1	0	63	NA2	S-08	6	68	40				
		S-01	6	1	1	64		S-10	3	73	42				
		S01-03	2	0	0	71		S-11	6	74	43				
α3/α6	Lac	S01-03	6	0	0	72	S-12	29	79	44					
		S-01	-1	0	0	42	S-01	1	16	19	68				
		S04-01	-1	0	0	70	S-03	33	18	69					
α6-α8	Lac	S01-04	0	0	0	71	S-04	7	35	70					
		S03-01	0	0	0	69	S-05	1	21	37	71				
		S-01	2	1	0	41	S-07	1	51	63	72				
N/A	LNT	S-01	4	0	1	66	S-09	1	3	20	73				
		S01(03)	2	0	1	67	S-11	1	3	36	74				
		S01(04)	0	0	1	68	S-13	1	16	24	75				
N/A	LacNAc	S-01	2	0	0	73	S-14	1	33	21	76				
		S-05	3	0	57	37	S-15	1	41	65	77				
		S-06	3	1	35	38	S-01	0	7	57	1				
N/A	LacNAc	S-03	2	1	19	20	S-02	1	3	0	2				
		S-01	3	1	37	17	S-03	1	5	47	3				
		S-06	9	2	3	24	S-04	1	18	58	4				
N/A	GalNAc	S-05	6	1	98	3	S-05	2	35	95	5				
		S-06	9	1	82	4	S-06	15	70	6					
		S-03	6	1	58	18	S-07	2	18	64	7				
N/A	Gal	S-01	3	1	37	17	S-08	3	55	8					
		S-06	9	2	3	24	S-09	1	3	59	9				
		S-05	3	1	2	23	S-10	4	30	68	10				
N/A	Gal	S-03	8	1	1	6	S-12	3	12	52	11				
		S-01	2	0	0	5	S-13	1	10	62	12				
		S-06	8	1	19	32	S-14	1	7	68	13				
N/A	Sc	S-05	6	1	12	31	S-15	2	21	62	14				
		S-03	7	1	9	28	S-16	6	58	100	15				
		S-01	5	1	3	27	S-01	1	2	30	31				
N/A	LNT	S-01	13	1	14	53	S-03	1	3	29	32				
		S-01	1	1	0	59	S-01	1	3	3	79				
		Lac	11	1	1	43	NA2	0	0	80					
N/A	LacNAc	LacNAc	64	1	1	45	Man5	-2	0	80					
		GalNAc	13	2	1	47	LNT	0	53	0	78				
		Gal	16	1	1	49	Sc	0	0	80					
N/A	Core1	Core1	7	2	2	51									
		6S-LacNAc	10	1	0	54									

FIGURE 1. **Selective recognition of sialoglycans by plant lectins.** Biotinylated lectins were assayed using the protocol optimized for Array 1 (as detailed under “Experimental Procedures”) and detected with 1.5 μg/ml Cy3-streptavidin. *a*, selective recognition of Siaα2–6-glycans by biotinylated-SNA (tested at 20 μg/ml, Scanner 2). *b* and *c*, differential selective recognition of Siaα2–3-glycans by MAL-1 (*b*) and MAL-2 (*c*) to both arrays (tested at 40 μg/ml, Scanner 2). *d*, ranked binding of all plant lectins on both arrays. Binding of biotinylated lectins to the arrays tested at two or three concentrations (in the linear binding range for each scanner: Array 1, Scanner 1 at 40 and 20 μg/ml; Array 2, Scanner 2 at 20, 2, and 0.2 μg/ml for SNA and 40, 4, and 0.4 μg/ml for MAL-1/2). This binding was ranked as the percentage of maximal signal in each array (rank = 100 × (glycan RFU/RFU maximum at each concentration)), and the relative rankings were then averaged to obtain the average rank of each glycan. Each lectin average rank is presented as a heat map (red, white, and blue represent the maximum, 50th percentile, and minimum, respectively).

12, 11, 1, and 2 ranked 100, 31, 30, and 27, respectively), which is destabilized when the underlying glycan is sulfated (Siaα2–3-6S-LacNAc; glycan 12 versus 62 ranked 100 and 6, respectively). By contrast, Array 2 showed stronger binding with

MAL-1 specifically for Siaα2–3-glycan and underlying glycan preference toward LNnT or NA2 (Fig. 1*b*). These structures share the common terminal motif Siaα2–3Galβ1–4GlcNAcβ-R (Siaα2–3LacNAc) that is also the preferred epitope on Array 1.

## Cross-comparison of Two Sialoglycan Microarrays

The lower level of binding to Array 1 compared with Array 2 may result from various factors. Possibilities include the additional underlying glycan structures on Array 2 (the most likely reason), a different presentation of this binding motif (farther away from the slide surface, less dense, more mobile), and/or physical differences in slide coating on epoxide- and NHS-derivatized slides. MAL-1 does not bind to Sia $\alpha$ 2-3LNT, which is consistent with its preference toward  $\beta$ 1-4-linked galactosides, such as LNnT/NA2, over  $\beta$ 1-3-linked galactosides, such as LNT (Fig. 1*d*). In addition, MAL-1 does not bind to Sia $\alpha$ 2-3Lactose, consistent with its preference for an underlying LacNAc structure (Fig. 1*d*). As with SNA, modifications of the terminal Sia also affect MAL-1 binding to Array 2 sialoglycans; the top five ranked glycans on the LNnT skeleton showed optimal binding to the modified Sias, including Kdn5,9Ac<sub>2</sub>, Neu5Ac9Me, Neu5Ac8Me, Kdn5Ac, and Kdn7Me (glycans 30, 23, 17, 29, and 26 ranked 95, 80, 72, 70, and 62) and significantly lower binding to their corresponding unmodified Sias, such as Kdn and Neu5Ac (glycans 19 and 16 ranked 28 and 23). Overall, the binding pattern is similar to previous analysis conducted with different buffer conditions (11).

In contrast to MAL-1, MAL-2 showed stronger binding to Array 1 than to Array 2 (Fig. 1*c*). On Array 1, MAL-2 binds mostly to Sia $\alpha$ 2-3Core1 (Sia $\alpha$ 2-3Gal $\beta$ 1-3GalNAc), with no binding even to the very similar glycans with a Type 1 underlying skeleton (Sia $\alpha$ 2-3Gal $\beta$ 1-3GlcNAc, differing only at the position C-4 of the last monosaccharide) (Fig. 1*d*). Furthermore, the linker attached to the reducing end of the trisaccharide dramatically affected the binding efficiency, showing a clear preference toward the  $\alpha$ -linkage (glycans 16, 15, 9, and 10,  $\alpha$ -linked, ranked 100, 67, 66, and 38; glycans 33-36,  $\beta$ -linked, ranked 5-10; Fig. 1*d*). A comparable binding pattern was observed when the same slide was scanned and analyzed with two different scanners (supplemental Fig. 1*b*;  $R^2 = 0.92$ ). These findings suggest that the optimal ligand for MAL-2 is Sia $\alpha$ 2-3Gal $\beta$ 1-3GalNAc1 $\alpha$ -R (Sia $\alpha$ 2-3Core1 $\alpha$ -R). It also raises the possibility that the binding might be further stabilized with additional glycans or amino acids at the reducing end; however, this would need to be tested. The lack of Sia $\alpha$ 2-3Core1 $\alpha$ -R on Array 2 provides a logical explanation for the lack of MAL-2 binding on this array.

Some lectins require divalent cations for optimal binding. We therefore assayed MAL-2 on Array 1 with Buffer 2 (BisTris, pH 6.0, 1 mM Ca<sup>2+</sup>, 1 mM Mg<sup>2+</sup>, 150 mM NaCl), which was supplemented with 1% ovalbumin for blocking and lectin binding or supplemented with 0.1% Tween for washing. MAL-2 showed the same preference toward Sia $\alpha$ 2-3Core1 $\alpha$ -R as with Buffer 1 (PBS with 1% ovalbumin). However, the change in buffer further broadened the binding to sialoglycans with other underlying glycans, such as Sia $\alpha$ 2-3Type1 and Sia $\alpha$ 2-3Gal (supplemental Fig. 2*a*), and with an overall stronger signal in each glycan (by ~5-fold; supplemental Fig. 2*b*). However, these buffer conditions did not affect the binding intensity or pattern of SNA (supplemental Fig. 2*b*) and did not improve on low binding of MAL-1 to Array 1 (data not shown).

In summary, the direct comparison of both arrays by these common sialic acid-binding lectins showed interesting differences that can be interpreted as due to suboptimal pres-

entation of glycans and/or physical differences in the slide surfaces (as in the differences in MAL-1 binding to its ligand, Sia $\alpha$ 2-3Gal $\beta$ 1-4GlcNAc, on the two arrays) and/or due to the absence of optimal ligand (the absence of the structure Neu5Gc $\alpha$ 2-3Gal $\beta$ 1-3GalNAc $\alpha$ 1-R on Array 2). This is an excellent example of how the number, diversity, and presentation of glycans on an array can affect the specificity determination of a GBP.

*Differential Impact of Sialic Acid C-5 Variations on Sialoglycan Recognition by Polyclonal and Monoclonal Anti-Neu5Gc Antibodies*—Binding of several antibodies with reported anti-Neu5Gc specificity was assayed on both arrays (with the buffers and conditions optimized for Array 1; see “Experimental Procedures”), and the binding patterns to the sialoglycans were compared. These antibodies showed differential selective recognition on the two arrays (Fig. 2, *a-d*), including an affinity-purified polyclonal chicken anti-Neu5Gc IgY (pChGc) (33) and two monoclonal chicken anti-Neu5Gc IgYs (mChGc6-1 and mChGc2-7) (34). On Array 1, the polyclonal antibody pChGc recognition was not greatly affected by the various underlying skeletons or the terminal sialyl linkages and showed an overall strong and specific binding to all sialoglycans with terminal Neu5Gc or their 9-*O*-acetylated derivatives (Fig. 2, *a* and *d*, ranked 52-94), except for two glycans (glycans 72 and 73 ranked 7 and 2, respectively) in which Neu5Gc is internal (Neu5Ac $\alpha$ 8Neu5Gc $\alpha$ 3/6Lac). By contrast, on Array 2, binding was affected by the various underlying skeletons, the terminal sialyl linkages, and most significantly, the Sia type. On Array 2, this polyclonal pChGc antibody preferentially bound to sialoglycans with unmodified Neu5Gc (ranked 100 to 24) or Neu5GcOAc with *O*-acetylation on the glycolyl (ranked 75 to 12) and showed very weak or no binding to 9-*O*-acetylated Neu5Gc (ranked 6 to 0) and lack of binding to glycans with *O*-methylation on the glycolyl in Neu5Gc (Neu5GcOMe; Fig. 2, *a* and *d*), indicating selective recognition of the sialoglycans through position 5. Thus, evaluation of data from each array allows an interpretation of the specificity of this polyclonal antibody, and the conclusions are complementary. Despite clear relative differences in pChGc binding between each array, the data are in overall agreement that this antibody has a strict specificity for terminal Neu5Gc and most or all of its extended glycan derivatives. The nature of the factors that create the observed differences in binding is unknown but may be related to the differences in the derivatized surfaces, packing density, and/or mobility/conformation of the glycans.

Similarly, the two anti-Neu5Gc monoclonal antibodies, mChGc6-1 and mChGc2-7, showed differential recognition on the two arrays with strong binding to Array 1 and low binding to Array 2 (Fig. 2, *b* and *c*), with all scanners tested (supplemental Fig. 1*b*). On Array 1, both monoclonal antibodies did not bind glycan structures with internal Neu5Gc (Fig. 2*d*; glycans 72 and 73), similar to pChGc. mChGc6-1 showed greater binding to unmodified Neu5Gc-glycans over the 9-*O*-acetylated ones with a preference toward Sia $\alpha$ 2-3 over Sia $\alpha$ 2-6 or Sia $\alpha$ 2-8 linkages to the underlying skeletons with an almost complete lack of binding to 9-*O*-acetylated Neu5Gc $\alpha$ 2-6 and minimal binding to the GD3-like glycan 69 (Neu5Gc $\alpha$ 2-8Neu5Ac $\alpha$ 2-3Gal $\beta$ 1-



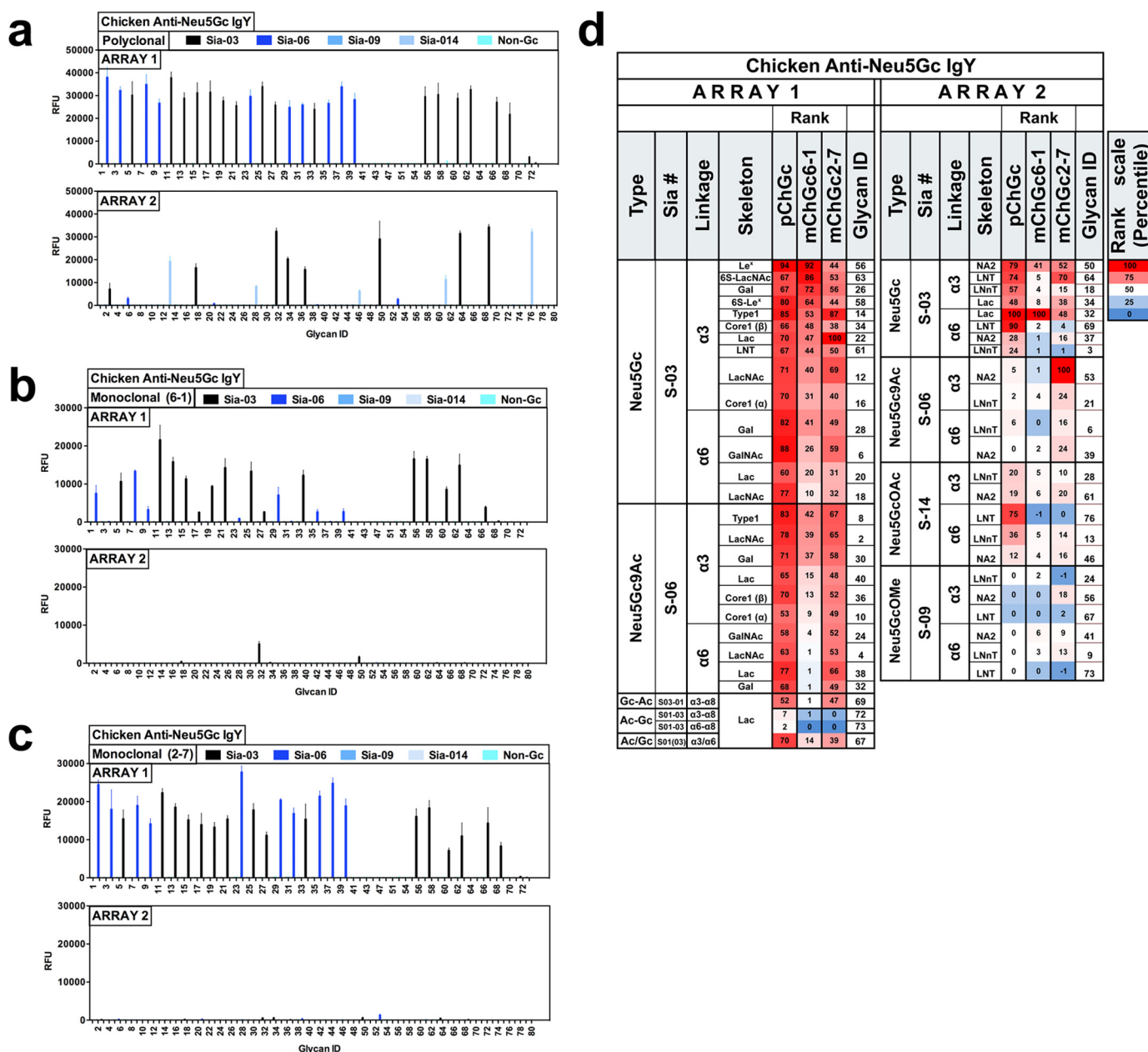


FIGURE 2. Selective recognition of sialoglycans by specific antibodies. Chicken IgY anti-Neu5Gc antibodies were assayed using the protocol optimized for Array 1 and detected with 1.5  $\mu$ g/ml Cy3-donkey anti-chicken IgY. *a*, selective recognition of Neu5Gc-bearing glycans by monospecific chicken polyclonal anti-Neu5Gc antibodies to both arrays (tested at 1:10,000 dilution, Scanner 2). *b* and *c*, differential selective recognition of Neu5Gc-bearing glycans by two chicken monoclonal anti-Neu5Gc antibodies on both arrays (hybridoma supernatant tested at 1:50 dilution, Scanner 2). *d*, average ranked binding (as detailed in the legend to Fig. 1*d*) of anti-Neu5Gc antibodies on both arrays tested at two concentrations each (in the linear binding range of Scanner 1: polyclonal anti-Neu5Gc IgY at 1:10,000 and 1:20,000 dilutions; monoclonal anti-Neu5Gc IgY at 1:250 and 1:500 dilutions). The average rank is presented as a heat map of all tested glycans, and only the Neu5Gc-glycoconjugates are presented (red, white, and blue represent the maximum, 50th percentile, and minimum, respectively).

4Glc $\beta$ -R; Fig. 2*d*). This antibody also showed variation in underlying glycan recognition, although there is some sensitivity to the  $\alpha/\beta$ -linkage of the glycan-linker because the  $\alpha$ -linkage is preferred in Sia $\alpha 2$ -3Core1 $\alpha/\beta$ -R structures (glycan 34 versus 16 ranked 48 versus 31, and glycan 36 versus 10 ranked 13 versus 9; Fig. 2*d*). On Array 2, this antibody showed minimal binding and mostly bound to Neu5Gc-glycans with unmodified Sia. The second monoclonal antibody mChGc2-7 resembled pChGc and showed a broader binding profile on both arrays compared with mChGc6-1 (Fig. 2, *b-d*). On both arrays, mChGc2-7 bound to both Neu5Gc-glycans and their modified derivatives

with a modest preference for Sia $\alpha 2$ -3 over Sia $\alpha 2$ -6 linkage. On Array 2, in contrast to pChGc or mChGc6-1, mChGc2-7 showed strong binding to 9-O-acetylated Sia. The differential binding patterns of mChGc6-1 and mChGc2-7 to the two arrays may result from differential presentation of Neu5Gc-glycans on the two arrays that might negatively affect stable binding to Array 2. For example, less dense and more mobile glycans might reduce bivalent binding.

Selective Recognition of Sialoglycans with O-Acetylated Sialic Acids—Coronaviruses are a group of enveloped (+) strand RNA viruses and include the severe acute respiratory syndrome

## Cross-comparison of Two Sialoglycan Microarrays

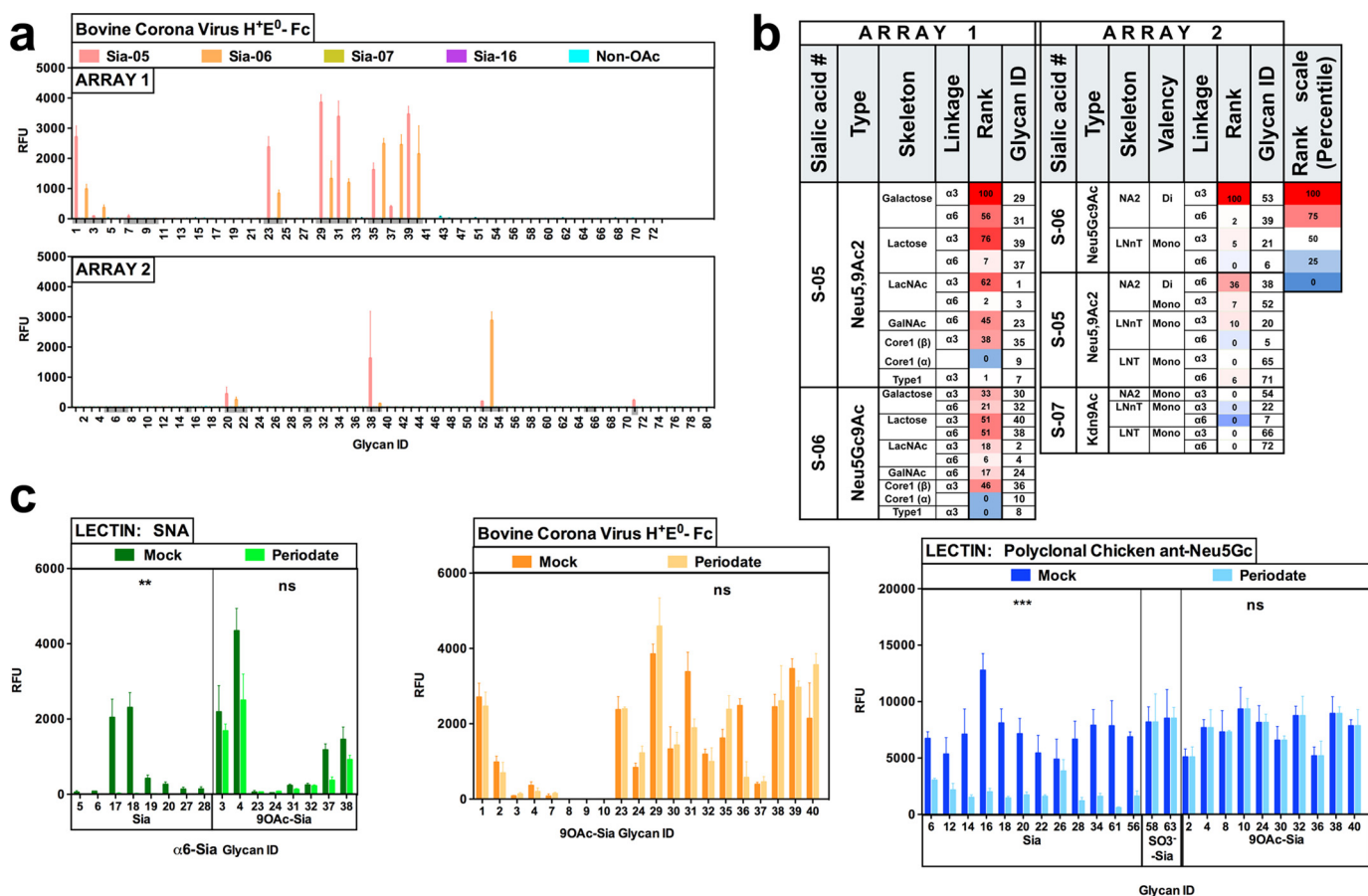


**FIGURE 3. Selective recognition of glycans bearing O-acetyl-modified sialic acids.** *a*, selective recognition of 9-*O*-acetylated Sias (9OAc-Sia) by the viral lectin BCoV H<sup>+</sup>E<sup>0</sup>-Fc, an Fc fusion protein of bovine coronavirus hemagglutinin-esterase (*HE*) ectodomain with an inactivated esterase (35) was tested at 50 and 40 μg/ml (Array 1 and Array 2, respectively, Scanner 1). *b*, average ranked binding of BCoV H<sup>+</sup>E<sup>0</sup>-Fc to 9OAc-Sia on both arrays (*c*). Specificity for sialic acid (validated by mild periodate treatment). Pretreatment of arrays with freshly prepared 2 mM sodium metaperiodate in PBS, pH 6.5, but not mock treatment (as detailed under "Experimental Procedures") abolishes binding of lectins and antibodies to unmodified sialoglycans (Sia); however, this treatment does not abolish binding to 9OAc-Sia, which is protected from mild periodate oxidation. Shown is binding to periodate or mock-treated arrays with biotinylated SNA at 20 μg/ml (*left*), BCoV H<sup>+</sup>E<sup>0</sup>-Fc at 50 μg/ml (*middle*), and polyclonal anti-Neu5Gc IgY at 1:10,000 dilution (*right*).

coronavirus and bovine coronavirus (BCoV). BCoVs use 9-*O*-acetylated sialic acids as receptors and correspondingly possess sialate-9-*O*-acetylsterases as receptor-destroying enzymes (39, 40). To demonstrate the analytical power of the arrays in selective recognition of 9-*O*-acetylated Sias, we tested the viral lectin BCoV H<sup>+</sup>E<sup>0</sup>-Fc, an Fc fusion protein of the bovine coronavirus hemagglutinin-esterase ectodomain (residues 19–388) with an inactivated esterase (H<sup>+</sup>E<sup>0</sup>, containing a Ser<sup>40</sup> → Ala substitution in the active site (35)). Fig. 3*a* shows the binding pattern of this viral lectin to both arrays demonstrating differentially selective recognition. On Array 1, the preferred ligands have a terminal 9-*O*-acetylated Sia, with preference toward Neu5,9Ac<sub>2</sub> over Neu5Gc9Ac (rank range 100 to 0 versus 51 to 0; Fig. 3*b*) and Siaα<sub>2</sub>–3 linkage over Siaα<sub>2</sub>–6. The underlying skeleton similarly affected binding, showing clear preference for Gal according to Gal > Lac > LacNAc > GalNAc > Core 1 and complete lack of binding to Siaα<sub>2</sub>–3Type1. In addition, binding shows sensitivity to the α/β-linkage of the linker with preference for the β-linkage as in Siaα<sub>2</sub>–3Core1α/β-R structures (glycan 35 versus 9 ranked 37.8 versus 0, and glycan 36 versus 10 ranked 46 versus 0; Fig. 3*b*). That is in contrast to MAL-2 that prefers the α-linkage on the same glycans (Fig. 1*d*).

Similarly, on Array 2, binding of the viral lectin BCoV H<sup>+</sup>E<sup>0</sup>-Fc shows that the preferred ligand has terminal 9-*O*-acetylated Sia with preference toward Siaα<sub>2</sub>–3 linkage over Siaα<sub>2</sub>–6 (glycan 53 versus 39 ranked 100 versus 1.6, glycan 21 versus 6 ranked 5.3 versus 0, and glycan 20 versus 5 ranked 9.8 versus 0; Fig. 3*b*). In monovalent presentation, Neu5,9Ac<sub>2</sub> is preferred over Neu5Gc9Ac (Neu5,9Ac<sub>2</sub>α<sub>2</sub>–3LNnT is preferred over Neu5Gc9Acα<sub>2</sub>–3LNnT; glycan 20 versus 21 ranked 9.8 versus 5.3) but shows no binding to the mono-9OAc-Siaα<sub>2</sub>–6LNnT). Interestingly, binding to divalent glycans bearing 9OAc-Sia was better than to any of the monovalent glycans with Neu5Gc9Acα<sub>2</sub>–3NA2 (glycan 53) ranked 100 and Neu5,9Ac<sub>2</sub>α<sub>2</sub>–6NA2 (glycan 38) ranked 35.6, suggesting that the linkage effect on binding is stronger than the Sia type. Binding to sialoglycans with LNT skeleton was very low (Neu5,9Ac<sub>2</sub>α<sub>2</sub>–3/6LNT glycans 35/71 ranked 0/5.6); similarly, no binding to sialoglycans with Type 1 glycan on Array 1 was detected, suggesting that the underlying common motif (Galβ1–3GlcNAc) is not optimal for binding. On Array 2, no binding was observed for sialoglycans with other types of modified Sia (such as Kdn9Ac or Kdn5,9Ac<sub>2</sub>, Neu5Ac9Me, and Neu5Ac9Lt), indicating that the 5-acetyl/glycolyl groups also

contribute to the recognition by this lectin in addition to the 9-*O*-acetyl modification.

**Mild Periodate Oxidation for Evaluating Sialoglycan Binding Specificity**—To confirm Sia-specific binding, glycans on the slides were treated with mild periodate oxidation, which would specifically truncate the polyhydroxyl side chain of Sia, leaving a reactive aldehyde that is then further reduced by sodium borohydride, thus generating a terminal hydroxyl at carbon 7. The resulting modified Sia has two fewer hydroxyl group-attached carbons (carbons 8 and 9) but maintains the Sia negative charge. This allows investigation of the specificity for sialic acid itself as opposed to simply a charged monosaccharide. An exception is the 9-*O*-acetylated Sia (9OAc-Sia), which is resistant to such periodate oxidation (41), thereby leaving the 9OAc-Sia intact and further indicating its specific recognition. Considering the fact that 9OAc-Sia is better preserved under mild acidic conditions (42), we optimized the periodate oxidation protocol accordingly and found that 2 mM periodate in PBS, pH 6.5, provides better stability compared with conventional sodium acetate, pH 5.5 (data not shown). The optimal periodate concentration was 2 mM, with further increases resulting in glycan degradation (data not shown). As shown in Fig. 3c, mild periodate oxidation (2 mM in PBS, pH 6.5) of Array 1 completely abolishes binding of SNA to sialylated glycans with C-9-unprotected sialic acid compared with the mock-treated array, whereas the binding to the resistant 9OAc-Sia remains largely unchanged, indicating Sia-specific and 9OAc-Sia-specific binding, respectively, through the Sia side chain. In keeping with this, periodate treatment did not reduce binding of the viral lectin BCoV H<sup>+</sup>E<sup>0</sup>-Fc compared with the mock-treated array (Fig. 3c), supporting its specificity toward 9OAc-Sia. Likewise, the polyclonal chicken anti-Neu5Gc antibody (pChGc) shows reduction in binding to periodate-treated Sia except for 9OAc-Sia (Fig. 3c). Surprisingly, pChGc analysis further revealed that, similar to 9OAc-Sia, the Neu5Gc-containing sulfated glycans (such as 6S-Le<sup>x</sup> and 6S-LacNAc) retain binding even after periodate treatment, suggesting either protection of the terminal unmodified Sia from periodate oxidation or that pChGc can still bind to the truncated Sia while stabilized by the sulfated groups in these glycans. Such glycans (Neu5Gcα1-3Galβ1-4(Fuca1-3)GlcNAc6Sβ-R glycan 58 and Neu5Gcα1-3Galβ1-4GlcNAc6Sβ-R glycan 63, periodate-resistant) showed resistance to periodate treatment compared with sialoglycans with the corresponding non-sulfated skeletons (number 56 and 12, periodate-sensitive). Overall, this approach allows an independent assessment of sialic acid specificity of GBPs as well as an evaluation of the stability of 9-*O*-acetyl substitutions.

**Differential Array Recognition by Human Sialic Acid-binding Lectins CHL-1 and Siglec-9**—To expand our comparison, we also tested some animal lectins with known Sia-dependent binding on both arrays. L1 and the close homolog of L1 (CHL1) are immunoglobulin (Ig) class transmembrane receptors with critical functions in neurodevelopment. Members of the L1 family of neural cell adhesion molecules (L1-CAMs) are widely expressed in the developing nervous system and regulate axon guidance and synaptic plasticity (43). It was reported that CD24 and L1 cooperate with each other through binding of L1 to α2-3-linked Sias on CD24, thereby contributing to neurite out-

growth (44, 45). We tested human Fc-fusion proteins of both L1 (36) and CHL1 (37) for binding to glycans on both arrays using the optimal Buffer 2 conditions. Although both L1-Fc and CHL1-Fc showed a dose-dependent binding to sialylated CD24 by traditional ELISA (supplemental Fig. 3a), they showed very weak binding to both arrays (CHL1-Fc; supplemental Fig. 3b) (data not shown). On Array 1, CHL1 binding was not Sia-dependent, whereas on Array 2, there was very weak binding to divalent (glycans 39 and 50) or short monovalent glycans (Siaα2-3/6Lac, glycans 31 and 34), with some preference for the monovalent Siaα2-3LNT, especially with several modified Sias (supplemental Fig. 3c; Kdn9Ac > Neu5,9Ac<sub>2</sub> > Neu5GcOMe on Type 1 underlying glycans) and lower binding to Siaα2-6LNnT. Overall, this is another example where two arrays that present diverse sets of sialosides do not show strong binding by a GBP that is known to recognize Sias in a biological context (supplemental Fig. 3b). Possible explanations include lack of an unknown optimal binding ligand found only on CD24, contribution of a CD24 peptide component to binding (such as occurs with P-selectin recognition of PSGL-1 (46)), or failure to mimic a unique “clustered saccharide patch” (47) that may be found on CD24.

We also tested an Fc fusion protein of human Siglec-9 (38), which is known to recognize Sias (Siglecs are sialic acid-recognizing immunoglobulin-like lectins). In contrast to L1-Fc/CHL1-Fc, human Siglec-9-Fc showed very low binding to Array 2, which does not allow delineation of a binding motif, but strong binding to Array 1 (Fig. 4, a–c). On Array 1, binding is sensitive to Sia type, Sia linkage, underlying glycan structure, and the linkage and length of the glycan linker. This was reproduced in both laboratories using a range of concentrations (0.1–40 μg/ml as related to the scanners' sensitivities; Fig. 4, b and c), two different secondary antibodies, and two different scanners (Cy3-goat anti-human IgG on Scanner 1 and Alexa Fluor 633-goat anti-human IgG on Scanner 2; Fig. 4, b and c) yet yielding quite similar binding patterns (Fig. 4, b and c). Human Siglec-9-Fc shows preference for Kdn-containing glycans (even if internal) and for unmodified Sia (non-9-*O*-acetylated) and Siaα2-6 linkage on several skeletons. 6-*O*-Sulfation of the underlying skeleton increases binding, revealing Sia-6S-Le<sup>x</sup> > sLe<sup>x</sup> and Sia-6S-LacNAc > Sia-LacNAc preference (Fig. 4b).

Binding of human Siglec-9-Fc to Array 1 Core 1 structures showed that the linkage of the trisaccharide to the linker dramatically affected the binding efficiency (Fig. 4b), revealing a clear preference for the β-linkage (glycans 33–36, β-linked, ranked 52–57; glycans 16, 15, 9, and 10, α-linked, ranked 18 to 0; Cy3-goat anti-human IgG; Fig. 4b and supplemental Fig. 2c). This preference for the β-linkage of the linker is also observed with the viral lectin BCoV H<sup>+</sup>E<sup>0</sup>-Fc (Fig. 3b) but is in contrast to MAL-2 (Fig. 1d and supplemental Fig. 2c). In addition, human Siglec-9-Fc showed a strong preference for unmodified Sia (glycan 33 *versus* 35 ranked 39 *versus* 7; glycan 34 *versus* 36 ranked 52 *versus* 10). Furthermore, binding was abolished when a longer linker (Linker-01 *versus* Linker-02, Table 3) was used to conjugate the glycans to the slide on Array 1 (glycan 41 *versus* 64 or glycan 42 *versus* 65). Similarly, very low binding was observed for the longer pentasaccharides, such as the sialylated LNT (glycans 60 and 61), which is in contrast to the very high

# Cross-comparison of Two Sialoglycan Microarrays

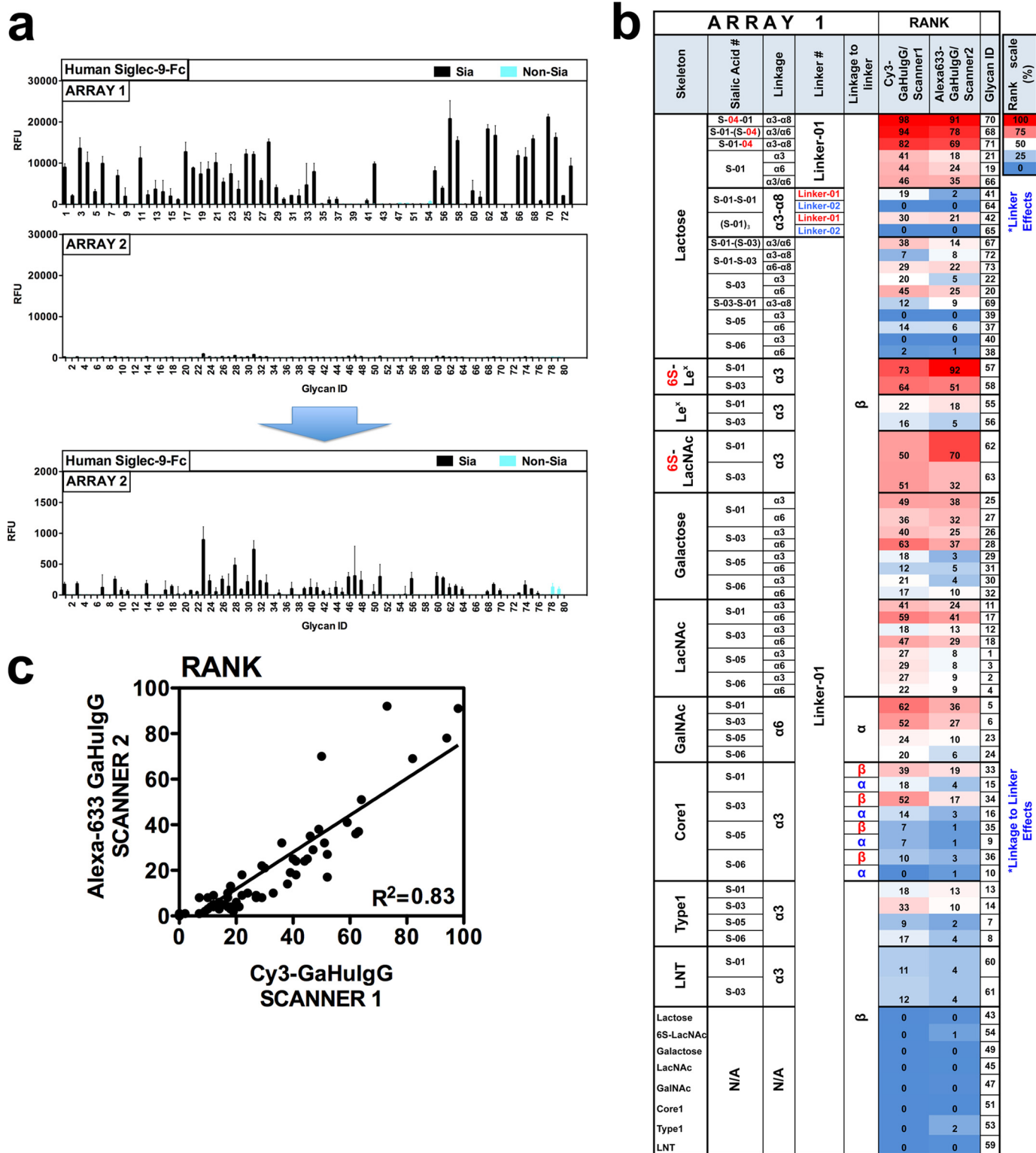


**FIGURE 4. Differential recognition of sialoglycans by human Siglec-9.** Lectins were assayed using the protocol optimized for Array 1 and detected with 1.5  $\mu\text{g/ml}$  Cy3-goat anti-human IgG. *a*, binding of the human Siglec-9-Fc chimera to both arrays was assayed using the protocol optimized for Array 1 and detected with 1.5  $\mu\text{g/ml}$  Cy3-goat anti-human IgG (tested at 40  $\mu\text{g/ml}$  on both arrays, Scanner 2). *b*, average ranked binding (as detailed in the legend to Fig. 1d) of human Siglec-9-Fc to Array 1 developed either with 1.5  $\mu\text{g/ml}$  Cy3-goat anti-human IgG (tested in the linear binding range of Scanner 1 at 20 and 40  $\mu\text{g/ml}$ ) or with 1.5  $\mu\text{g/ml}$  Alexa Fluor 633-goat anti-human IgG (tested in the linear binding range of Scanner 2 at 1 and 0.1  $\mu\text{g/ml}$ ). The average rank is presented as a heat map of all tested glycans (red, white, and blue represent the maximum, 50th percentile, and minimum, respectively). Of note, as indicated in the figure (\*), Array 1 has two examples of di-/trisialylated probes that differ only in the glycan linker (short versus long) used for immobilization (glycans 41 versus 64 or glycan 42 versus 65; Table 3) as well as four sialylated Core 1 glycans carrying the same linker that is differentially attached to the glycan probes ( $\beta$ -linked: glycans 33–36 versus  $\alpha$ -linked: glycans 16, 15, 9, and 10; Table 1). Both differences (the linkage or length of the glycan linker) had dramatically and differentially affected the binding efficiencies of human Siglec-9 (summarized in supplemental Fig. 2c). *c*, direct comparison of the calculated average rank for Array 1 as obtained in *b*.

binding to this Neu5Gc-containing glycan (glycan 61) by all of the tested anti-Neu5Gc antibodies (Fig. 2*d*). This may suggest that the binding of this animal lectin, human Siglec-9-Fc, is specifically negatively affected by the flexibility of the glycans on the printed array.

These data demonstrate that whereas the binding of human Siglec-9-Fc is specific to various sialoglycans, it is also sensitive to the linkage and length of the glycan linker attaching the glycoconjugate to the slide surface. This differential recognition with stronger and wider recognition by Array 1 compared with Array 2 is hence probably due to the different presentation of glycans on the arrays, due to factors such as the open or closed ring structure of the reducing sugar (diagram in Table 3), the length and the stereo-specificity of the linker, and/or printing chemistry (Table 3). In this regard, it is interesting that the differences between the two arrays were in the opposite direction compared with the plant lectin MAL-1 that showed strong binding to Array 2 and low binding to Array 1 (Fig. 1*b*). Taken together, binding of human Siglec-9 shows differential binding on Array 1 compared with Array 2. However, even within the same array, we observe a differential binding pattern as a result of differential immobilization chemistries.

When defined glycan microarrays are being interrogated with GBPs of unknown specificity, any binding observed may represent a cross-reaction of the GBP with a glycan related to its natural ligand. Thus, the differential binding of human Siglec-9 to Arrays 1 and 2 may be a result of the protein cross-reacting with all Sias with a preference for the tandem repeats containing Kdn and sulfated sialyl-Le<sup>x</sup> glycans on Array 1. However, the interaction of Siglec-9 with Array 2 terminal Sias may be less stabilized due to the differences in linkers and NHS-derivatized substrate. In addition, the low binding to Array 2 may be due to the absence of the preferred glycans. This is consistent with other comparisons where Array 2 and Array 1 generate the same broad specificity determination; *i.e.* both arrays showed specificity of anti-Neu5Gc antibodies for Neu5Gc-terminating glycans, but Array 2 with lower binding levels demonstrated the antibody's preference for different derivatives of Neu5Gc and linkage position to underlying structures. This is also consistent with the behavior of human Siglec-9 on other arrays, all showing the preferred binding specificity for sulfated sialyl-Le<sup>x</sup> and related glycans; *e.g.* on the Feizi neoglycolipids array (48), on the Consortium for Functional Glycomics NeutrAvidin plate array (384-well glycanarrays v3.2 and v3.4), and on the Consortium for Functional Glycomics mammalian cell glycan array (data not shown), where glycans are printed on NHS-derivatized surfaces as in Array 2 (6) (note that tandem repeats of Sias containing Kdn are not currently found on the Consortium for Functional Glycomics array).

*Direct Comparisons of Recognition of Compounds with Common Terminal Glycans on the Two Arrays*—Many but not all of the differences between the two arrays can be attributed to specific differences in the actual structures of the glycans. To better address the differential recognition, we directly compared the binding to the six pairs of glycans that share the same terminal di- or trisaccharide on both arrays (supplemental Table 1; ranked 0) but differ in their immobilization chemistries

(Table 3 and Fig. 5*b*). For this comparison, we evaluated binding of human Siglec-9-Fc and the three chicken anti-Neu5Gc IgYs and ranked these pairs binding to each array (Fig. 5, *a* and *b*). Such analyses indicate that in certain cases, there is no direct correlation with relative binding of glycan pairs, despite the fact that they share the same terminal structures (Fig. 5, *a* and *c*). Such differences between these arrays may be due to many factors, such as differential behavior of proteins on the epoxide *versus* NHS-derived slides. Indeed, if Array 2 glycans are printed on epoxy slides, Siglec-9 binds with broad specificity at higher concentrations (data not shown), similar to the findings with Array 1. Other additional factors could generate differences in presentation of glycans for binding to GBPs, including the effect of the open chain monosaccharide at the reducing end and different linkers (Table 3).

*Conclusions and Perspectives*—To generate a tractable cross-platform comparison, we compare two relatively extensive glycan arrays that are based on the family of sialic acids with analysis mainly focused on terminal glycan motif recognition. This study demonstrates the power of glycan microarrays in analyzing GBP binding to the diversity of sialoglycans in nature. Comparisons of GBP binding within individual arrays are meaningful when glycans are presented at the same concentration and coupled with the same chemistry. However, this first ever direct cross-comparison of glycan arrays suggests that mining of data in current glycan array databases derived from different platforms (different chemistries and substrates) should be done with caution. Our initial cross-comparison highlights many possible factors that can contribute to differential recognition of glycan arrays, including diversity in glycan attachment chemistries, array processing protocols, and the extent of coverage of the glycan library. However, at this point, it is very difficult to generalize conclusions for every possible case. We believe that such general conclusions should rely on a larger data volume that would include cross-comparison assays with additional platforms. More specifically, at least in the case of human Siglec-9 and despite the great differences we observe between the two compared arrays, when glycan recognition is compared with other published array data, it seems that, when a strong binding ligand is present on an array, the different immobilization chemistries will not completely eliminate its detection. However, this may not be the case with lower binding ligands. It would be interesting to conduct comprehensive cross-comparison analyses on some other widely used glycan arrays (6).

Unlike the well standardized nucleic acid microarrays and some protein microarrays, glycan microarray data should be viewed as experiments and not definitive assays because no glycan array at present embodies a complete glycome or even all of the predicted glycan determinants (49), which precludes being able to make conclusions regarding the natural ligand of a given GBP. This is analogous to the limitations of gene microarrays comprised of a collection of nucleic acid sequences from a small, random fraction of the human genome. Furthermore, glycan arrays have several other levels of complexity. The diversity of the glycome may be further expanded by its three-dimensional organization, involving “clustered saccharide patches” (47, 50) or “mixed glycan epitopes” (51), when neigh-

## Cross-comparison of Two Sialoglycan Microarrays

**a**

Lectin	Conc	PAIRS	Glycan ID (ARRAY1/ARRAY2)	Compound on Array 1	Related Compounds on Array 2	ARRAY1 RFU	ARRAY2 RFU	ARRAY1 RANK	ARRAY2 RANK	
Human Siglec-9Fc	20 µg/ml	PAIR-1	21/33	Neu5Acα3Galβ4GlcβO(CH <sub>2</sub> ) <sub>2</sub> CH <sub>2</sub> NH <sub>2</sub>	Neu5Acα3Galβ4Glcitol-AEAB	1896	0	28	0	
		PAIR-2	19/31	Neu5Acα6Galβ4GlcβO(CH <sub>2</sub> ) <sub>2</sub> CH <sub>2</sub> NH <sub>2</sub>	Neu5Acα6Galβ4Glcitol-AEAB	6714	0	100	0	
		PAIR-3	22/34	Neu5Gca3Galβ4GlcβO(CH <sub>2</sub> ) <sub>2</sub> CH <sub>2</sub> NH <sub>2</sub>	Neu5Gca3Galβ4Glcitol-AEAB	317	0	5	0	
		PAIR-4	20/32	Neu5Gca6Galβ4GlcβO(CH <sub>2</sub> ) <sub>2</sub> CH <sub>2</sub> NH <sub>2</sub>	Neu5Gca6Galβ4Glcitol-AEAB	1787	113	27	100	
		PAIR-5	60/63	Neu5Acα3Galβ3GlcNacβ3Galβ4GlcβO(CH <sub>2</sub> ) <sub>2</sub> CH <sub>2</sub> NH <sub>2</sub>	Neu5Acα3Galβ3GlcNacβ3Galβ4Glcitol-AEAB	1218	35	18	31	
		PAIR-6	61/64	Neu5Gca3Galβ3GlcNacβ3Galβ4GlcβO(CH <sub>2</sub> ) <sub>2</sub> CH <sub>2</sub> NH <sub>2</sub>	Neu5Gca3Galβ3GlcNacβ3Galβ4Glcitol-AEAB	5707	21	85	19	
	40 µg/ml	PAIR-1	21/33	Neu5Acα3Galβ4GlcβO(CH <sub>2</sub> ) <sub>2</sub> CH <sub>2</sub> NH <sub>2</sub>	Neu5Acα3Galβ4Glcitol-AEAB	10076	193	100	26	
		PAIR-2	19/31	Neu5Acα6Galβ4GlcβO(CH <sub>2</sub> ) <sub>2</sub> CH <sub>2</sub> NH <sub>2</sub>	Neu5Acα6Galβ4Glcitol-AEAB	7292	736	72	100	
		PAIR-3	22/34	Neu5Gca3Galβ4GlcβO(CH <sub>2</sub> ) <sub>2</sub> CH <sub>2</sub> NH <sub>2</sub>	Neu5Gca3Galβ4Glcitol-AEAB	5321	0	53	0	
		PAIR-4	20/32	Neu5Gca6Galβ4GlcβO(CH <sub>2</sub> ) <sub>2</sub> CH <sub>2</sub> NH <sub>2</sub>	Neu5Gca6Galβ4Glcitol-AEAB	8449	226	84	31	
		PAIR-5	60/63	Neu5Acα3Galβ3GlcNacβ3Galβ4GlcβO(CH <sub>2</sub> ) <sub>2</sub> CH <sub>2</sub> NH <sub>2</sub>	Neu5Acα3Galβ3GlcNacβ3Galβ4Glcitol-AEAB	3211	138	32	19	
		PAIR-6	61/64	Neu5Gca3Galβ3GlcNacβ3Galβ4GlcβO(CH <sub>2</sub> ) <sub>2</sub> CH <sub>2</sub> NH <sub>2</sub>	Neu5Gca3Galβ3GlcNacβ3Galβ4Glcitol-AEAB	1656	85	16	12	
Chicken anti-Neu5Gc Ig y	Polyclonal (6-1)	1:10,000	PAIR-3	22/34	Neu5Gca3Galβ4GlcβO(CH <sub>2</sub> ) <sub>2</sub> CH <sub>2</sub> NH <sub>2</sub>	Neu5Gca3Galβ4Glcitol-AEAB	25604	20314	89	63
			PAIR-4	20/32	Neu5Gca6Galβ4GlcβO(CH <sub>2</sub> ) <sub>2</sub> CH <sub>2</sub> NH <sub>2</sub>	Neu5Gca6Galβ4Glcitol-AEAB	27756	32418	96	100
			PAIR-6	61/64	Neu5Gca3Galβ3GlcNacβ3Galβ4GlcβO(CH <sub>2</sub> ) <sub>2</sub> CH <sub>2</sub> NH <sub>2</sub>	Neu5Gca3Galβ3GlcNacβ3Galβ4Glcitol-AEAB	28829	31445	100	97
	Monoclonal (2-7)	1:50	PAIR-3	22/34	Neu5Gca3Galβ4GlcβO(CH <sub>2</sub> ) <sub>2</sub> CH <sub>2</sub> NH <sub>2</sub>	Neu5Gca3Galβ4Glcitol-AEAB	14264	158	100	3
			PAIR-4	20/32	Neu5Gca6Galβ4GlcβO(CH <sub>2</sub> ) <sub>2</sub> CH <sub>2</sub> NH <sub>2</sub>	Neu5Gca6Galβ4Glcitol-AEAB	9333	5020	65	100
			PAIR-6	61/64	Neu5Gca3Galβ3GlcNacβ3Galβ4GlcβO(CH <sub>2</sub> ) <sub>2</sub> CH <sub>2</sub> NH <sub>2</sub>	Neu5Gca3Galβ3GlcNacβ3Galβ4Glcitol-AEAB	8532	88	60	2
Monoclonal (2-7)	1:50	PAIR-3	22/34	Neu5Gca3Galβ4GlcβO(CH <sub>2</sub> ) <sub>2</sub> CH <sub>2</sub> NH <sub>2</sub>	Neu5Gca3Galβ4Glcitol-AEAB	15396	597	100	100	
		PAIR-4	20/32	Neu5Gca6Galβ4GlcβO(CH <sub>2</sub> ) <sub>2</sub> CH <sub>2</sub> NH <sub>2</sub>	Neu5Gca6Galβ4Glcitol-AEAB	13237	533	86	89	
		PAIR-6	61/64	Neu5Gca3Galβ3GlcNacβ3Galβ4GlcβO(CH <sub>2</sub> ) <sub>2</sub> CH <sub>2</sub> NH <sub>2</sub>	Neu5Gca3Galβ3GlcNacβ3Galβ4Glcitol-AEAB	7125	458	46	77	

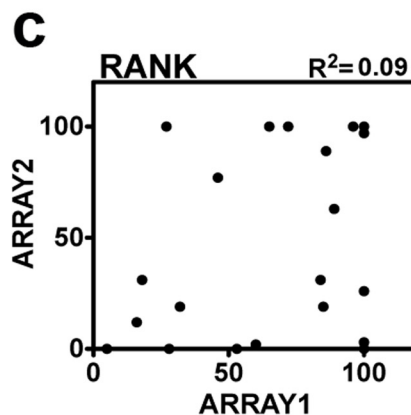
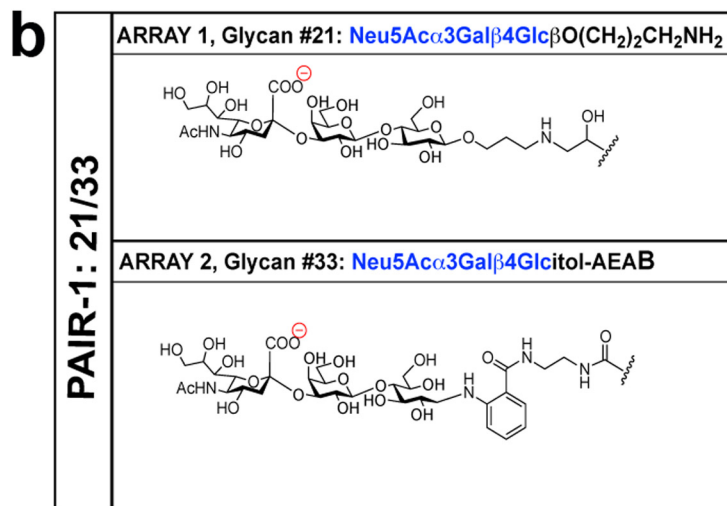


**FIGURE 5. Differential recognition of similar glycans on both arrays with the same lectins.** *a*, direct comparison of the RFU of lectins binding to pairs of highly similar sialoglycans on both arrays (glycan pairs with exact terminal structure but different linker and slide coat; Supplemental Table 1 and diagram in Table 3), as tested with human Siglec-9Fc and the various anti-Neu5Gc antibodies (data from Figs. 2 and 4). Binding was then ranked as the percentage of maximal binding for each lectin within the compared glycan pairs. *b*, schematic representation of one matched glycan pair on the two arrays (PAIR-1). *c*, direct comparison of the ranked glycan pairs for Array 1 versus Array 2 (goodness of fit estimated by linear regression).

boring glycans are presumed to interact with one another, to generate unique epitopes. For example, the three-dimensional organization of two combined gangliosides resulted in unique epitopes for anti-ganglioside antibodies (anti-GQ1b) (52). Likewise, it was recently shown that heterogeneous glycans, prepared by mixing two distinct oligosaccharides that are spotted onto glass slides, may result in enhanced binding affinity compared with the individual components in microarray experiments. Furthermore, the antibody binding avidity in such heterogeneous samples seemed to be influenced by the affinity and steric effects of neighboring glycans (51). Thus, glycan microarray data from indi-

vidual glycan microarrays must be analyzed and interpreted with respect to the collection of glycans on each array. The information generated can then be used to develop hypotheses with additional experiments on other arrays or in other formats to define the function of protein-glycan interactions and to identify the physiological ligand for the GBP in question.

*Acknowledgment*—We thank Jamie Heimburg-Molinaro (Emory University School of Medicine) for help in data management and manuscript preparation.

## REFERENCES

- Schena, M., Shalon, D., Davis, R. W., and Brown, P. O. (1995) Quantitative monitoring of gene expression patterns with a complementary DNA microarray. *Science* **270**, 467–470
- Lueking, A., Horn, M., Eickhoff, H., Büssow, K., Lehrach, H., and Walter, G. (1999) Protein microarrays for gene expression and antibody screening. *Anal. Biochem.* **270**, 103–111
- Trevino, V., Falciani, F., and Barrera-Saldaña, H. A. (2007) DNA microarrays. A powerful genomic tool for biomedical and clinical research. *Mol. Med.* **13**, 527–541
- Kricka, L. J., Master, S. R., Joos, T. O., and Fortina, P. (2006) Current perspectives in protein array technology. *Ann. Clin. Biochem.* **43**, 457–467
- Smith, D. F., Song, X., and Cummings, R. D. (2010) Use of glycan microarrays to explore specificity of glycan-binding proteins. *Methods Enzymol.* **480**, 417–444
- Rillahan, C. D., and Paulson, J. C. (2011) Glycan microarrays for decoding the glycome. *Annu. Rev. Biochem.* **80**, 797–823
- Oyularan, O., and Gildersleeve, J. C. (2009) Glycan arrays. Recent advances and future challenges. *Curr. Opin. Chem. Biol.* **13**, 406–413
- Fukui, S., Feizi, T., Galustian, C., Lawson, A. M., and Chai, W. (2002) Oligosaccharide microarrays for high-throughput detection and specificity assignments of carbohydrate-protein interactions. *Nat. Biotechnol.* **20**, 1011–1017
- Wang, D., Liu, S., Trummer, B. J., Deng, C., and Wang, A. (2002) Carbohydrate microarrays for the recognition of cross-reactive molecular markers of microbes and host cells. *Nat. Biotechnol.* **20**, 275–281
- Varki, A., and Lowe, J. B. (2009) In *Essentials of Glycobiology* (Varki, A., Cummings, R. D., Esko, J. D., Freeze, H. H., Stanley, P., Bertozzi, C. R., Hart, G. W., and Etzler, M. E., eds) Chapter 6, Cold Spring Harbor Laboratory, Cold Spring Harbor, NY
- Song, X., Yu, H., Chen, X., Lasanajak, Y., Tappert, M. M., Air, G. M., Tiwari, V. K., Cao, H., Chokhawala, H. A., Zheng, H., Cummings, R. D., and Smith, D. F. (2011) A sialylated glycan microarray reveals novel interactions of modified sialic acids with proteins and viruses. *J. Biol. Chem.* **286**, 31610–31622
- Van Damme, E. J., Smith, D. F., Cummings, R., and Peumans, W. J. (2011) Glycan arrays to decipher the specificity of plant lectins. *Adv. Exp. Med. Biol.* **705**, 757–767
- Song, X., Lasanajak, Y., Olson, L. J., Boonen, M., Dahms, N. M., Kornfeld, S., Cummings, R. D., and Smith, D. F. (2009) Glycan microarray analysis of P-type lectins reveals distinct phosphomannose glycan recognition. *J. Biol. Chem.* **284**, 35201–35214
- Bochner, B. S., Alvarez, R. A., Mehta, P., Bovin, N. V., Blixt, O., White, J. R., and Schnaar, R. L. (2005) Glycan array screening reveals a candidate ligand for Siglec-8. *J. Biol. Chem.* **280**, 4307–4312
- Padler-Karavani, V., Hurtado-Ziola, N., Pu, M., Yu, H., Huang, S., Muthana, S., Chokhawala, H. A., Cao, H., Secrest, P., Friedmann-Morvinski, D., Singer, O., Ghaderi, D., Verma, I. M., Liu, Y. T., Messer, K., Chen, X., Varki, A., and Schwab, R. (2011) Human xeno-autoantibodies against a non-human sialic acid serve as novel serum biomarkers and immunotherapeutics in cancer. *Cancer Res.* **71**, 3352–3363
- van Vliet, S. J., van Liempt, E., Saeland, E., Aarnoudse, C. A., Appelmelk, B., Irimura, T., Geijtenbeek, T. B., Blixt, O., Alvarez, R., van Die, I., and van Kooyk, Y. (2005) Carbohydrate profiling reveals a distinctive role for the C-type lectin MGL in the recognition of helminth parasites and tumor antigens by dendritic cells. *Int. Immunol.* **17**, 661–669
- Reis, C. A., Campos, D., Osório, H., and Santos, L. L. (2011) Glycopeptide microarray for autoantibody detection in cancer. *Expert Rev. Proteomics* **8**, 435–437
- MAQC Consortium, Shi, L., Reid, L. H., Jones, W. D., Shippy, R., Warrington, J. A., Baker, S. C., Collins, P. J., de Longueville, F., Kawasaki, E. S., Lee, K. Y., Luo, Y., Sun, Y. A., Willey, J. C., Setterquist, R. A., Fischer, G. M., Tong, W., Dragan, Y. P., Dix, D. J., Frueh, F. W., Goodsaid, F. M., Herman, D., Jensen, R. V., Johnson, C. D., Lobenhofer, E. K., Puri, R. K., Schrf, U., Thierry-Mieg, J., Wang, C., Wilson, M., Wolber, P. K., Zhang, L., Amur, S., Bao, W., Barbacioru, C. C., Lucas, A. B., Bertholet, V., Boysen, C., Bromley, B., Brown, D., Brunner, A., Canales, R., Cao, X. M., Cebula, T. A., Chen, J. J., Cheng, J., Chu, T. M., Chudin, E., Corson, J., Corton, J. C., Croner, L. J., Davies, C., Davison, T. S., Delenstarr, G., Deng, X., Dorris, D., Eklund, A. C., Fan, X. H., Fang, H., Fulmer-Smentek, S., Fuscoe, J. C., Gallagher, K., Ge, W., Guo, L., Guo, X., Hager, J., Haje, P. K., Han, J., Han, T., Harbottle, H. C., Harris, S. C., Hatchwell, E., Hauser, C. A., Hester, S., Hong, H., Hurban, P., Jackson, S. A., Ji, H., Knight, C. R., Kuo, W. P., LeClerc, J. E., Levy, S., Li, Q. Z., Liu, C., Liu, Y., Lombardi, M. J., Ma, Y., Magnuson, S. R., Maqsoodi, B., McDaniel, T., Mei, N., Myklebost, O., Ning, B., Novoradovskaya, N., Orr, M. S., Osborn, T. W., Papallo, A., Patterson, T. A., Perkins, R. G., Peters, E. H., Peterson, R., Phillips, K. L., Pine, P. S., Pusztai, L., Qian, F., Ren, H., Rosen, M., Rosenzweig, B. A., Samaha, R. R., Schena, M., Schroth, G. P., Shchegrova, S., Smith, D. D., Staedtler, F., Su, Z., Sun, H., Szallasi, Z., Tezak, Z., Thierry-Mieg, D., Thompson, K. L., Tikhonova, I., Turpaz, Y., Vallanat, B., Van, C., Walker, S. J., Wang, S. J., Wang, Y., Wolfinger, R., Wong, A., Wu, J., Xiao, C., Xie, Q., Xu, J., Yang, W., Zhang, L., Zhong, S., Zong, Y., and Slikker, W. J. (2006) The MicroArray Quality Control (MAQC) project shows inter- and intraplatform reproducibility of gene expression measurements. *Nat. Biotechnol.* **24**, 1151–1161
- Brazma, A., Hingamp, P., Quackenbush, J., Sherlock, G., Spellman, P., Stoeckert, C., Aach, J., Ansorge, W., Ball, C. A., Causton, H. C., Gaasterland, T., Glenisson, P., Holstege, F. C., Kim, I. F., Markowitz, V., Matese, J. C., Parkinson, H., Robinson, A., Sarkans, U., Schulze-Kremer, S., Stewart, J., Taylor, R., Vilo, J., and Vingron, M. (2001) Minimum information about a microarray experiment (MIAME). Toward standards for microarray data. *Nat. Genet.* **29**, 365–371
- Schauer, R., Srinivasan, G. V., Wipfler, D., Kniep, B., and Schwartz-Albiez, R. (2011) O-Acetylated sialic acids and their role in immune defense. *Adv. Exp. Med. Biol.* **705**, 525–548
- Varki, A., and Schauer, R. (2009) In *Essentials of Glycobiology* (Varki, A., Cummings, R. D., Esko, J. D., Freeze, H. H., Stanley, P., Bertozzi, C. R., Hart, G. W., and Etzler, M. E., eds) pp. 199–218, Cold Spring Harbor Laboratory, Cold Spring Harbor, NY
- Chen, X., and Varki, A. (2010) Advances in the biology and chemistry of sialic acids. *ACS Chem. Biol.* **5**, 163–176
- Yu, H., Cao, H., Tiwari, V. K., Li, Y., and Chen, X. (2011) Chemoenzymatic synthesis of C8-modified sialic acids and related  $\alpha$ 2–3- and  $\alpha$ 2–6-linked sialosides. *Bioorg. Med. Chem. Lett.* **21**, 5037–5040
- Ding, L., Yu, H., Lau, K., Li, Y., Muthana, S., Wang, J., and Chen, X. (2011) Efficient chemoenzymatic synthesis of sialyl Tn antigen and derivatives. *Chem. Commun.* **47**, 8691–8693
- Cao, H., Muthana, S., Li, Y., Cheng, J., and Chen, X. (2009) Parallel chemoenzymatic synthesis of sialosides containing a C5-diversified sialic acid. *Bioorg. Med. Chem. Lett.* **19**, 5869–5871
- Yu, H., Chokhawala, H. A., Huang, S., and Chen, X. (2006) One-pot three-enzyme chemoenzymatic approach to the synthesis of sialosides containing natural and non-natural functionalities. *Nat. Protoc.* **1**, 2485–2492
- Yu, H., Cheng, J., Ding, L., Khedri, Z., Chen, Y., Chin, S., Lau, K., Tiwari, V. K., and Chen, X. (2009) Chemoenzymatic synthesis of GD3 oligosaccharides and other disialyl glycans containing natural and non-natural sialic acids. *J. Am. Chem. Soc.* **131**, 18467–18477
- Yu, H., Chokhawala, H., Karpel, R., Yu, H., Wu, B., Zhang, J., Zhang, Y., Jia, Q., and Chen, X. (2005) A multifunctional *Pasteurella multocida* sialyltransferase. A powerful tool for the synthesis of sialoside libraries. *J. Am. Chem. Soc.* **127**, 17618–17619
- Yu, H., Huang, S., Chokhawala, H., Sun, M., Zheng, H., and Chen, X. (2006) Highly efficient chemoenzymatic synthesis of naturally occurring and non-natural  $\alpha$ -2,6-linked sialosides. A *P. damsela*  $\alpha$ -2,6-sialyltransferase with extremely flexible donor-substrate specificity. *Angew. Chem. Int. Ed. Engl.* **45**, 3938–3944
- Chokhawala, H. A., Huang, S., Lau, K., Yu, H., Cheng, J., Thon, V., Hurtado-Ziola, N., Guerrero, J. A., Varki, A., and Chen, X. (2008) Combinatorial chemoenzymatic synthesis and high-throughput screening of sialosides. *ACS Chem. Biol.* **3**, 567–576
- Shengshu, H., Hai, Y., and Xi, C. (2011) Chemoenzymatic synthesis of  $\alpha$ 2–3-sialylated carbohydrate epitopes. *Sci. China Chem.* **54**, 117–128
- Lau, K., Yu, H., Thon, V., Khedri, Z., Leon, M. E., Tran, B. K., and Chen, X. (2011) Sequential two-step multienzyme synthesis of tumor-associated sialyl T-antigens and derivatives. *Org. Biomol. Chem.* **9**, 2784–2789

## Cross-comparison of Two Sialoglycan Microarrays

33. Diaz, S. L., Padler-Karavani, V., Ghaderi, D., Hurtado-Ziola, N., Yu, H., Chen, X., Brinkman-Van der Linden, E. C., Varki, A., and Varki, N. M. (2009) Sensitive and specific detection of the non-human sialic acid *N*-glycolylneuraminic acid in human tissues and biotherapeutic products. *PLoS ONE* **4**, e4241
34. Asaoka, H., Nishinaka, S., Wakamiya, N., Matsuda, H., and Murata, M. (1992) Two chicken monoclonal antibodies specific for heterophil Hanganutziu-Deicher antigens. *Immunol. Lett.* **32**, 91–96
35. Zeng, Q., Langereis, M. A., van Vliet, A. L., Huizinga, E. G., and de Groot, R. J. (2008) Structure of coronavirus hemagglutinin-esterase offers insight into corona and influenza virus evolution. *Proc. Natl. Acad. Sci. U.S.A.* **105**, 9065–9069
36. Roonprapunt, C., Huang, W., Grill, R., Friedlander, D., Grumet, M., Chen, S., Schachner, M., and Young, W. (2003) Soluble cell adhesion molecule L1-Fc promotes locomotor recovery in rats after spinal cord injury. *J. Neurotrauma* **20**, 871–882
37. Naus, S., Richter, M., Wildeboer, D., Moss, M., Schachner, M., and Bartsch, J. W. (2004) Ectodomain shedding of the neural recognition molecule CHL1 by the metalloprotease-disintegrin ADAM8 promotes neurite outgrowth and suppresses neuronal cell death. *J. Biol. Chem.* **279**, 16083–16090
38. Angata, T., and Varki, A. (2000) Cloning, characterization, and phylogenetic analysis of siglec-9, a new member of the CD33-related group of siglecs. Evidence for co-evolution with sialic acid synthesis pathways. *J. Biol. Chem.* **275**, 22127–22135
39. Vlasak, R., Luytjes, W., Spaan, W., and Palese, P. (1988) Human and bovine coronaviruses recognize sialic acid-containing receptors similar to those of influenza C viruses. *Proc. Natl. Acad. Sci. U.S.A.* **85**, 4526–4529
40. de Groot, R. J. (2006) Structure, function and evolution of the hemagglutinin-esterase proteins of corona- and toroviruses. *Glycoconj. J.* **23**, 59–72
41. Cheresh, D. A., Reisfeld, R. A., and Varki, A. (1984) *O*-Acetylation of disialoganglioside GD3 by human melanoma cells creates a unique antigenic determinant. *Science* **225**, 844–846
42. Varki, A., and Diaz, S. (1984) The release and purification of sialic acids from glycoconjugates. Methods to minimize the loss and migration of *O*-acetyl groups. *Anal. Biochem.* **137**, 236–247
43. Maness, P. F., and Schachner, M. (2007) Neural recognition molecules of the immunoglobulin superfamily. Signaling transducers of axon guidance and neuronal migration. *Nat. Neurosci.* **10**, 19–26
44. Kleene, R., Yang, H., Kutsche, M., and Schachner, M. (2001) The neural recognition molecule L1 is a sialic acid-binding lectin for CD24, which induces promotion and inhibition of neurite outgrowth. *J. Biol. Chem.* **276**, 21656–21663
45. Lieberoth, A., Splittstoesser, F., Katagihallimath, N., Jakovcevski, I., Loers, G., Ranscht, B., Karageos, D., Schachner, M., and Kleene, R. (2009) Lewis<sup>x</sup> and  $\alpha$ 2,3-sialyl glycans and their receptors TAG-1, Contactin, and L1 mediate CD24-dependent neurite outgrowth. *J. Neurosci.* **29**, 6677–6690
46. Leppänen, A., White, S. P., Helin, J., McEver, R. P., and Cummings, R. D. (2000) Binding of glycosulfopeptides to P-selectin requires stereospecific contributions of individual tyrosine sulfate and sugar residues. *J. Biol. Chem.* **275**, 39569–39578
47. Cohen, M., and Varki, A. (2010) The sialome. Far more than the sum of its parts. *OMICS* **14**, 455–464
48. Campanero-Rhodes, M. A., Childs, R. A., Kiso, M., Komba, S., Le Narvor, C., Warren, J., Otto, D., Crocker, P. R., and Feizi, T. (2006) Carbohydrate microarrays reveal sulfation as a modulator of siglec binding. *Biochem. Biophys. Res. Commun.* **344**, 1141–1146
49. Cummings, R. D. (2009) The repertoire of glycan determinants in the human glycome. *Mol. Biosyst.* **5**, 1087–1104
50. Varki, A. (1994) Selectin ligands. *Proc. Natl. Acad. Sci. U.S.A.* **91**, 7390–7397
51. Liang, C. H., Wang, S. K., Lin, C. W., Wang, C. C., Wong, C. H., and Wu, C. Y. (2011) Effects of neighboring glycans on antibody-carbohydrate interaction. *Angew Chem. Int. Ed. Engl.* **50**, 1608–1612
52. Ogawa, G., Kaida, K., Kusunoki, S., Ueda, M., Kimura, F., and Kamakura, K. (2009) Antibodies to ganglioside complexes consisting of asialo-GM1 and GQ1b or GT1a in Fisher and Guillain-Barré syndromes. *J. Neuroimmunol.* **214**, 125–127



April 23, 2012

*SUPPLEMENTARY INFORMATION*

Cross-Comparison of Protein Recognition of Sialic Acid Diversity  
on Two Novel Sialoglycan Microarrays\*

**Vered Padler-Karavani<sup>1#</sup>, Xuezheng Song<sup>2#</sup>, Hai Yu<sup>3</sup>, Nancy Hurtado-Ziola<sup>4</sup>, Shengshu Huang<sup>3</sup>, Saddam Muthana<sup>3</sup>, Harshal A. Chokhawala<sup>3</sup>, Jiansong Cheng<sup>3</sup>, Andrea Verhagen<sup>1</sup>, Martijn A. Langereis<sup>5</sup>, Ralf Kleene<sup>6</sup>, Melitta Schachner<sup>7</sup>, Raoul J. de Groot<sup>5</sup>, Yi Lasanajak<sup>2</sup>, Haruo Matsuda<sup>8</sup>, Richard Schwab<sup>1</sup>, Xi Chen<sup>3</sup>, David F. Smith<sup>2</sup>, Richard D. Cummings<sup>2</sup> and Ajit Varki<sup>1</sup>.**

<sup>1</sup>Department of Medicine and Cellular and Molecular Medicine, University of California, San Diego, 9500 Gilman Drive, La Jolla, CA 92093, USA; <sup>2</sup>Department of Biochemistry, Glycomics Center, Emory University School of Medicine, Atlanta, GA 30322; <sup>3</sup>Department of Chemistry, University of California, Davis, CA 95616, USA; <sup>4</sup>Sialix, Inc., Vista, CA 92081, USA; <sup>5</sup>Virology Division, Department of Infectious Diseases and Immunology, Faculty of Veterinary Medicine, Utrecht University, Utrecht, The Netherlands; <sup>6</sup>Zentrum für Molekulare Neurobiologie, Universitätsklinikum Hamburg-Eppendorf, 20246 Hamburg, Germany; <sup>7</sup>Department of Biomedical Engineering, Rutgers, The State University of New Jersey, Piscataway, NJ 08854, USA; and <sup>8</sup>Department of Molecular and Applied Bioscience, Graduate School of Biosphere Science, Hiroshima University, Hiroshima, Japan

#The contributions of the first two authors are equal.

\*Running title: *Cross-comparison of two sialoglycan microarrays*

To whom correspondence should be addressed: Ajit Varki, University of California, San Diego, 9500 Gilman Drive, La Jolla, California 92093-0687, USA, Tel: 858-534-2214, Fax: 858-534-5611, E-mail: avarki@ucsd.edu or Richard D. Cummings, Emory University School of Medicine, Atlanta, GA 30322, USA, Tel: 404-727-5962, Fax: 404-727-2738, E-mail: rdcummi@emory.edu

## Supplementary Information

**Supplementary Figure 1: Direct comparisons of the same array generated by two contact printers and analyzed with two scanners. (a)** Direct comparison of Array 1 generated by two contact printers: compounds were printed on epoxide-coated slides using two different contact printers (as detailed in methods) and binding of biotinylated-SNA was compared (tested at 20  $\mu\text{g/ml}$  and detected with 1.5  $\mu\text{g/ml}$  Cy3-streptavidin, Scanner 1; goodness of fit estimated by linear regression). **(b)** Direct comparison of the same array analyzed by two different scanners: binding to Array 1 was assayed with biotinylated lectins (SNA at 40  $\mu\text{g/ml}$ , MAL-1/2 at 40, 20  $\mu\text{g/ml}$ , polyclonal chicken anti-Neu5Gc IgY at 1:10,000 and 1:20,000, and polyclonal chicken anti-Neu5Gc IgY at 1:50, 1:250 and 1:500). The same slides were then scanned with both Scanner 1 and Scanner 2 (detailed in methods) and the generated RFU directly compared (goodness of fit estimated by linear regression).

**Supplementary Figure 2. Differential effect of buffer composition on sialoglycan recognition. (a)** Effect of buffers on selective recognition of Sia $\alpha$ 2-3-linked glycans by MAL-2. Biotinylated MAL-2 was assayed at 20  $\mu\text{g/ml}$  using the protocol optimized for Array 1 with Buffer 2 (as detailed in methods; Buffer 2: Bis-Tris pH 6, 1 mM Ca<sup>+2</sup>, 1 mM Mg<sup>+2</sup>, 150 mM NaCl; for blocking or lectin binding supplemented with 1% ovalbumin; for washing supplemented with 0.1% Tween) and detected with 1.5  $\mu\text{g/ml}$  Cy3-streptavidin (in Buffer 2, Scanner 1). **(b)** Differential effect of buffer composition on two selected lectins. Direct comparison of buffer composition on MAL-2 and SNA recognition both tested at 20  $\mu\text{g/ml}$  in Buffer 2 or Buffer 1 (as detailed in methods; Buffer 1: PBS pH 7.4; for blocking or lectin binding supplemented with 1% ovalbumin;

for washing supplemented with 0.1% Tween) and detected with 1.5 µg/ml Cy3-streptavidin (in Buffer 2 or 1, respectively; Scanner 1). **(c)** Linkage of trisaccharides to the linker affects binding efficiency of MAL-2 (rank reproduced from Fig. 1d) and human Siglec-9-Fc (rank reproduced from Fig. 4b).

**Supplementary Figure 3. Animal lectins bind their natural ligands in ELISA**

**binding assays but not by array. (a)** Binding of the soluble chimeric Fc dimers of the cell adhesion molecules L1 and CHL-1 (L1-Fc and CHL-1-Fc) to CD24 tested in triplicates by ELISA at 20 µg/ml and 40 µg/ml. Representative of two independent experiments and shows mean ± s.d. Statistical analysis by 2-way ANOVA with Bonferroni posttest (\* p<0.05; \*\* p<0.01). On the arrays, lectins were assayed using the protocol optimized for Array 1 and detected with 1.5 µg/ml Cy3-goat anti-human IgG. **(b)** Binding of the soluble chimeric Fc dimers of the cell adhesion molecules CHL-1 (CHL-1-Fc) to both arrays (tested at 40 µg/ml, Scanner 1). **(c)** Average ranked binding (as detailed in legend to Figure 1d) of CHL-1-Fc to Array 2 (tested in the linear binding range of Scanner 1 at 20 µg/ml and 40 µg/ml). The average rank is presented as a heat map of all tested glycans and only the top 10 bound glycoconjugates are presented (red, white and blue represent the maximum, 50<sup>th</sup> percentile and minimum, respectively).

**Supplementary Table 1:** List of compounds with common terminal glycans (blue) on the two sialoglycan arrays, ranked according to the relative difference in underlying glycan structure (the linkers and slide coats are different between the arrays): (0) Exact terminal structure, different linker and slide coat; (1) One non-overlapping underlying glycan; (2) Two non-overlapping underlying glycan; (3) Three or more non-overlapping underlying glycan.

## Supplementary Methods

**Array 1 Sialoglycan-microarray fabrication method 1.** Epoxide-derivatized Corning slides were purchased from Thermo Fisher Scientific (Pittsburgh, PA) and the arrays were printed as described (1) with SMT-S50, Classic silicon pins with 50x50  $\mu\text{m}$  tips from Parallel Synthesis Technologies (Santa Clara, CA) using a UCSF DeRisi Linear Servo Motor Microarrayer, generating  $\sim 70$   $\mu\text{m}$  diameter spots. Glycoconjugates (New Table 2 VPK 12/06/10) were distributed into a 384-well source plates using 8 replicate wells per sample and 5  $\mu\text{l}$  per well (Version 11P1). Each glycoconjugate was prepared at 100  $\mu\text{M}$  in an optimized print buffer (300 mM phosphate buffer, pH 8.4). To monitor printing quality we used replicate-wells of human IgG (Jackson ImmunoResearch) at 150  $\mu\text{g}/\text{ml}$  (in PBS) for each printing-pin. 8 pins were used, with each pin printing 6 replicate spots/well (by using the 384-well source plate 6 times), 24 spots/row with spacing of 180 mm. One complete array was printed with each pin generating 8 sub-array blocks on each slide (within approx 16 hours/ $\sim 100$  slides). The humidity level in the arraying room was maintained at about 70% during printing. Printed slides were left on arrayer deck overnight, allowing humidity to drop to ambient levels. Next, the print order of the slides was recorded (using Fine Tip Black lab marker from VWR) and slides were packed, vacuum-sealed and stored in a desiccant chamber at RT until used. Slides were printed in one batch of  $\sim 100$  slides.

**Array 1 Sialoglycan-microarray fabrication method 2.** Arrays were fabricated by KAMTEK Inc. (Gaithersburg, MD). Epoxide-derivatized Corning slides were purchased from Thermo Fisher Scientific (Pittsburgh, PA). Glycoconjugates were distributed into six 384-well source plates (12-16 samples per plate) using 4 replicate wells per sample

and 20  $\mu$ l per well (Version 12). Each glycoconjugate was prepared at 100  $\mu$ M in an optimized print buffer (300 mM phosphate buffer, pH 8.4). To monitor printing quality, replicate-wells of human IgG (Jackson ImmunoResearch, at 150  $\mu$ g/ml) and Alexa-555 (25ng/ $\mu$ l) in print buffer were used for each printing run. The arrays were printed with four SMP5B (Array It). These are quill pins with bubble uptake channel and gives spot diameter of  $\sim$ 160 $\mu$ m (glycan spots  $\sim$  70  $\mu$ m). Printing was done using VersArray ChipWriter Pro (Virtek/BioRad). There is one super grid cluster on X-axis and two on Y-axis generating 8 sub-array blocks on each slide. Blotting was done (5 blots/dip; Blot Time: 0.05 secs) in order to have uniform sample distribution. Each grid (sub-array) has 16 spots/row, 20 columns with spot to spot spacing of 225  $\mu$ m. The humidity level in the arraying chamber was maintained at about 66% during printing. Printed slides were left on arrayer deck over-night, allowing humidity to drop to ambient levels (40-45%). Next, slides were packed, vacuum-sealed and stored in a desiccant chamber at RT until used. Slides were printed in one batch of 45 slides.

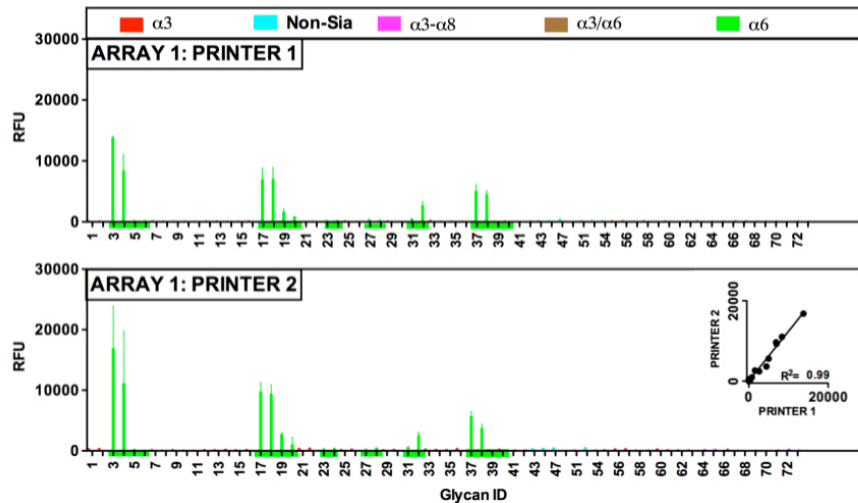
**ELISA.** Binding of L1 and CHL1 to CD24 was tested by ELISA as described (2), with several modifications. CD24 was purified as described (3) and coated in triplicates at 250 ng/well in TBS (50 mM Tris-buffer pH8, 150 mM NaCl) onto 96-well microtiter plates (Costar, Corning, NY) and plates were incubated overnight at 4°C. Wells were blocked for 1 hour at room temperature with Buffer 2 (Bis-Tris pH6, 1 mM Ca<sup>+2</sup>, 1 mM Mg<sup>+2</sup>, 150 mM NaCl) containing 1% ovalbumin (Grade V, Sigma) in PBS pH 7.4. Well were aspirated then incubated with diluted L1-Fc or CHL-1-Fc samples in the same blocking solution for 2 hours at room temperature. The plates were washed three times with Buffer 2 containing 0.1% Tween and subsequently incubated for 1 hour at room temperature

with HRP-conjugated goat-anti-human IgG (H+L; Bio-Rad, Hercules, CA) diluted 1:7000 in PBS. After washing three times with Buffer 2 containing 0.1% Tween, wells were developed with 140 µl of *O*-phenylenediamine in a citrate-PO<sub>4</sub> buffer, pH 5.5, and the reaction stopped with 40 µl of 4M of H<sub>2</sub>SO<sub>4</sub>. Absorbance was measured at a 490 nm wavelength on a SpectraMax 250 (Molecular Devices, Sunnyvale, CA). Specific binding was defined by subtracting the background readings obtained with the secondary antibody only on coated wells.

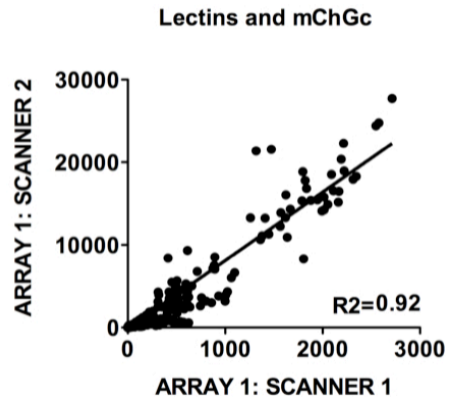
### References

1. Padler-Karavani, V., Hurtado-Ziola, N., Pu, M., Yu, H., Huang, S., Muthana, S., Chokhawala, H. A., Cao, H., Secret, P., Friedmann-Morvinski, D., Singer, O., Ghaderi, D., Verma, I. M., Liu, Y. T., Messer, K., Chen, X., Varki, A. and Schwab, R. (2011) *Cancer Res* **71**, 3352-3363
2. Padler-Karavani, V., Yu, H., Cao, H., Chokhawala, H., Karp, F., Varki, N., Chen, X. and Varki, A. (2008) *Glycobiology* **18**, 818-830
3. Kleene, R., Yang, H., Kutsche, M. and Schachner, M. (2001) *J Biol Chem* **276**, 21656-21663

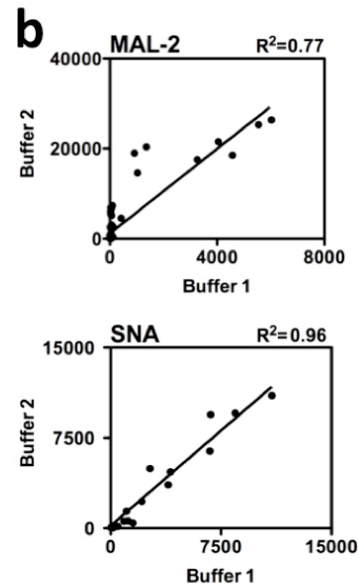
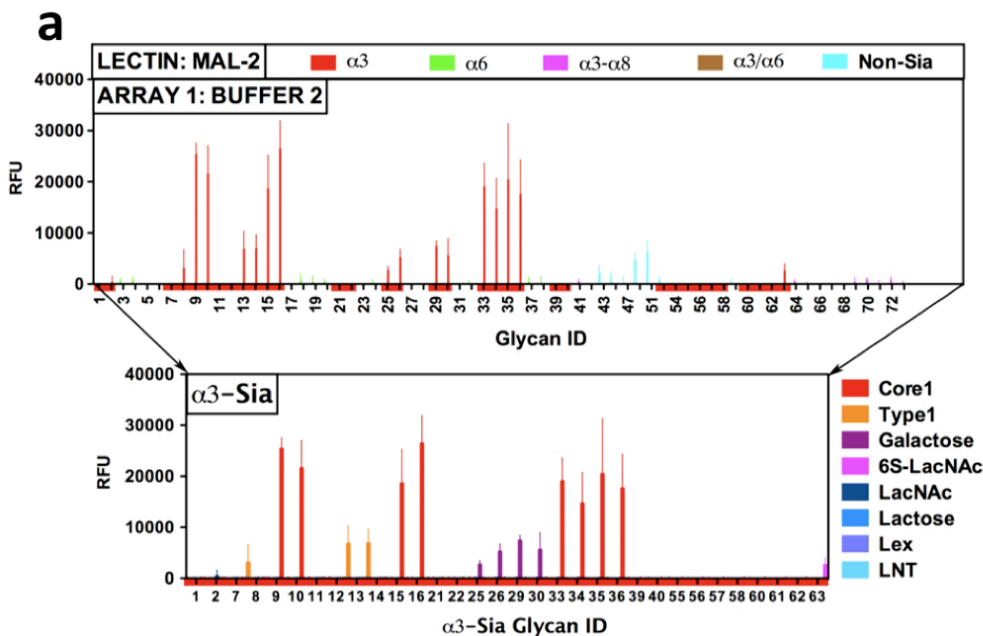
**a**



**b**





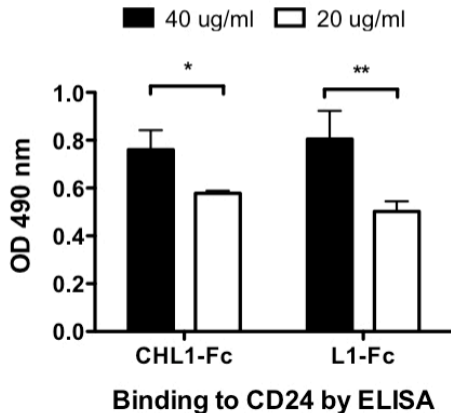


**c**

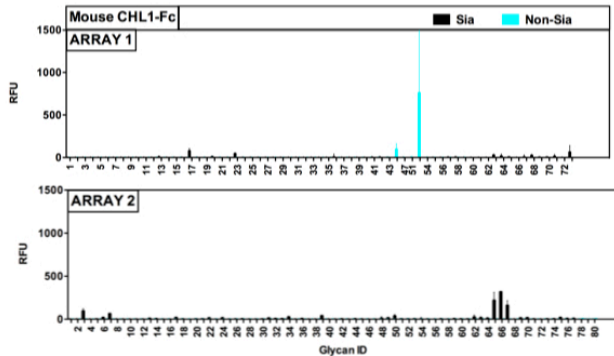
ARRAY 1							
Linkage	Skeleton	Sia #	Linkage to linker	Rank			Glycan ID
				MAL-2	Cy3- GaHugG/ Scanner1	Alexa633- GaHugG/ Scanner2	
					Human Siglec-9 Fc		
$\alpha 3$	Core1	$\beta$	S-01	5	39	19	33
			S-03	6	52	17	34
			S-05	10	7	1	35
		S-06	38	10	3	36	
		S-01	67	18	4	15	
		S-03	109	14	3	16	
	$\alpha$	$\alpha$	S-05	66	7	1	9
			S-06	36	6	1	10

# Padler-Karavani et al. Supplementary Figure 3

**a**



**b**



**c**

ARRAY 2				
Skeleton	Linkage	Sia #	Rank	
			CHL-1	Glycan ID
LNT	$\alpha 3$	Sia-07	100	66
		Sia-05	84	65
		Sia-09	50	67
LNnT	$\alpha 6$	Sia-03	32	3
		Sia-07	24	7
		Sia-05	6	5
NA2	$\alpha 3$	Sia-03	6	50
	$\alpha 6$	Sia-06	7	39
Lac	$\alpha 3$	Sia-03	4	34
	$\alpha 6$	Sia-01	5	31

Rank scale (%): 100 (red), 75 (orange), 50 (yellow), 25 (light blue), 0 (dark blue)

# Padler-Karavani et al. Supplementary Table 1

ARRAY 1			ARRAY 2		
EPOXY-COATED SLIDES			NHS-COATED SLIDES		
ID	Compound on Array 1	ID	Related Compounds on Array 2	Difference rank	
21	Neu5Aca3Galβ4GlcβO(CH <sub>2</sub> ) <sub>2</sub> CH <sub>2</sub> NH <sub>2</sub>	33	Neu5Aca3Galβ4Glcitol-AEAB	0	
19	Neu5Aca6Galβ4GlcβO(CH <sub>2</sub> ) <sub>2</sub> CH <sub>2</sub> NH <sub>2</sub>	31	Neu5Aca6Galβ4Glcitol-AEAB	0	
22	Neu5Gca3Galβ4GlcβO(CH <sub>2</sub> ) <sub>2</sub> CH <sub>2</sub> NH <sub>2</sub>	34	Neu5Gca3Galβ4Glcitol-AEAB	0	
20	Neu5Gca6Galβ4GlcβO(CH <sub>2</sub> ) <sub>2</sub> CH <sub>2</sub> NH <sub>2</sub>	32	Neu5Gca6Galβ4Glcitol-AEAB	0	
60	Neu5Aca3Galβ3GlcNacβ3Galβ4GlcβO(CH <sub>2</sub> ) <sub>2</sub> CH <sub>2</sub> NH <sub>2</sub>	63	Neu5Aca3Galβ3GlcNacβ3Galβ4Glcitol-AEAB	0	
61	Neu5Gca3Galβ3GlcNacβ3Galβ4GlcβO(CH <sub>2</sub> ) <sub>2</sub> CH <sub>2</sub> NH <sub>2</sub>	64	Neu5Gca3Galβ3GlcNacβ3Galβ4Glcitol-AEAB	0	
25	Neu5Aca3GalβO(CH <sub>2</sub> ) <sub>2</sub> CH <sub>2</sub> NH <sub>2</sub>	33	Neu5Aca3Galβ4Glcitol-AEAB	1	
27	Neu5Aca6GalβO(CH <sub>2</sub> ) <sub>2</sub> CH <sub>2</sub> NH <sub>2</sub>	31	Neu5Aca6Galβ4Glcitol-AEAB	1	
13	Neu5Aca3Galβ3GlcNacβO(CH <sub>2</sub> ) <sub>2</sub> CH <sub>2</sub> NH <sub>2</sub>	63	Neu5Aca3Galβ3GlcNacβ3Galβ4Glcitol-AEAB	2	
14	Neu5Gca3Galβ3GlcNacβO(CH <sub>2</sub> ) <sub>2</sub> CH <sub>2</sub> NH <sub>2</sub>	64	Neu5Gca3Galβ3GlcNacβ3Galβ4Glcitol-AEAB	2	
7	Neu5.9Ac <sub>2</sub> α3Galβ3GlcNacβO(CH <sub>2</sub> ) <sub>2</sub> CH <sub>2</sub> NH <sub>2</sub>	65	Neu5.9Ac <sub>2</sub> α3Galβ3GlcNacβ3Galβ4Glcitol-AEAB	2	
11	Neu5Aca3Galβ4GlcNacβO(CH <sub>2</sub> ) <sub>2</sub> CH <sub>2</sub> NH <sub>2</sub>	16	Neu5Aca3Galβ4GlcNacβ3Galβ4Glcitol-AEAB	2	
12	Neu5Gca3Galβ4GlcNacβO(CH <sub>2</sub> ) <sub>2</sub> CH <sub>2</sub> NH <sub>2</sub>	18	Neu5Gca3Galβ4GlcNacβ3Galβ4Glcitol-AEAB	2	
1	Neu5.9Ac <sub>2</sub> α3Galβ4GlcNacβO(CH <sub>2</sub> ) <sub>2</sub> CH <sub>2</sub> NH <sub>2</sub>	20	Neu5.9Ac <sub>2</sub> α3Galβ4GlcNacβ3Galβ4Glcitol-AEAB	2	
2	Neu5Gc9Aca3Galβ4GlcNacβO(CH <sub>2</sub> ) <sub>2</sub> CH <sub>2</sub> NH <sub>2</sub>	21	Neu5Gc9Aca3Galβ4GlcNacβ3Galβ4Glcitol-AEAB	2	
17	Neu5Aca6Galβ4GlcNacβO(CH <sub>2</sub> ) <sub>2</sub> CH <sub>2</sub> NH <sub>2</sub>	1	Neu5Aca6Galβ4GlcNacβ3Galβ4Glcitol-AEAB	2	
18	Neu5Gca6Galβ4GlcNacβO(CH <sub>2</sub> ) <sub>2</sub> CH <sub>2</sub> NH <sub>2</sub>	3	Neu5Gca6Galβ4GlcNacβ3Galβ4Glcitol-AEAB	2	
3	Neu5.9Ac <sub>2</sub> α6Galβ4GlcNacβO(CH <sub>2</sub> ) <sub>2</sub> CH <sub>2</sub> NH <sub>2</sub>	5	Neu5.9Ac <sub>2</sub> α6Galβ4GlcNacβ3Galβ4Glcitol-AEAB	2	
4	Neu5Gc9Aca6Galβ4GlcNacβO(CH <sub>2</sub> ) <sub>2</sub> CH <sub>2</sub> NH <sub>2</sub>	6	Neu5Gc9Aca6Galβ4GlcNacβ3Galβ4Glcitol-AEAB	2	
25	Neu5Aca3GalβO(CH <sub>2</sub> ) <sub>2</sub> CH <sub>2</sub> NH <sub>2</sub>	16	Neu5Aca3Galβ4GlcNacβ3Galβ4Glcitol-AEAB	3	
25	Neu5Aca3GalβO(CH <sub>2</sub> ) <sub>2</sub> CH <sub>2</sub> NH <sub>2</sub>	48	Neu5Aca3Galβ4GlcNacβ2Mana3(Neu5Aca3Galβ4GlcNacβ2Mana6)Manβ4GlcNacβ4GlcNacitol-AEAB	3	
25	Neu5Aca3GalβO(CH <sub>2</sub> ) <sub>2</sub> CH <sub>2</sub> NH <sub>2</sub>	63	Neu5Aca3Galβ3GlcNacβ3Galβ4Glcitol-AEAB	3	
26	Neu5Gca3GalβO(CH <sub>2</sub> ) <sub>2</sub> CH <sub>2</sub> NH <sub>2</sub>	18	Neu5Gca3Galβ4GlcNacβ3Galβ4Glcitol-AEAB	3	
26	Neu5Gca3GalβO(CH <sub>2</sub> ) <sub>2</sub> CH <sub>2</sub> NH <sub>2</sub>	50	Neu5Gca3Galβ4GlcNacβ2Mana3(Neu5Gca3Galβ4GlcNacβ2Mana6)Manβ4GlcNacβ4GlcNacitol-AEAB	3	
26	Neu5Gca3GalβO(CH <sub>2</sub> ) <sub>2</sub> CH <sub>2</sub> NH <sub>2</sub>	64	Neu5Gca3Galβ3GlcNacβ3Galβ4Glcitol-AEAB	3	
29	Neu5.9Ac <sub>2</sub> α3GalβO(CH <sub>2</sub> ) <sub>2</sub> CH <sub>2</sub> NH <sub>2</sub>	20	Neu5.9Ac <sub>2</sub> α3Galβ4GlcNacβ3Galβ4Glcitol-AEAB	3	
29	Neu5.9Ac <sub>2</sub> α3GalβO(CH <sub>2</sub> ) <sub>2</sub> CH <sub>2</sub> NH <sub>2</sub>	52	* Neu5.9Ac <sub>2</sub> α3Galβ4GlcNacβ2Mana3(Galβ4GlcNacβ2Mana6)Manβ4GlcNacβ4GlcNacitol-AEAB	3	
29	Neu5.9Ac <sub>2</sub> α3GalβO(CH <sub>2</sub> ) <sub>2</sub> CH <sub>2</sub> NH <sub>2</sub>	65	Neu5.9Ac <sub>2</sub> α3Galβ3GlcNacβ3Galβ4Glcitol-AEAB	3	
30	Neu5Gc9Aca3GalβO(CH <sub>2</sub> ) <sub>2</sub> CH <sub>2</sub> NH <sub>2</sub>	21	Neu5Gc9Aca3Galβ4GlcNacβ3Galβ4Glcitol-AEAB	3	
30	Neu5Gc9Aca3GalβO(CH <sub>2</sub> ) <sub>2</sub> CH <sub>2</sub> NH <sub>2</sub>	53	Neu5Gc9Aca3Galβ4GlcNacβ2Mana3(Neu5Gc9Aca3Galβ4GlcNacβ2Mana6)Manβ4GlcNacβ4GlcNacitol-AEAB	3	
27	Neu5Aca6GalβO(CH <sub>2</sub> ) <sub>2</sub> CH <sub>2</sub> NH <sub>2</sub>	1	Neu5Aca6Galβ4GlcNacβ3Galβ4Glcitol-AEAB	3	
27	Neu5Aca6GalβO(CH <sub>2</sub> ) <sub>2</sub> CH <sub>2</sub> NH <sub>2</sub>	35	Neu5Aca6Galβ4GlcNacβ2Mana3(Neu5Aca6Galβ4GlcNacβ2Mana6)Manβ4GlcNacβ4GlcNacitol-AEAB	3	
28	Neu5Gca6GalβO(CH <sub>2</sub> ) <sub>2</sub> CH <sub>2</sub> NH <sub>2</sub>	3	Neu5Gca6Galβ4GlcNacβ3Galβ4Glcitol-AEAB	3	
28	Neu5Gca6GalβO(CH <sub>2</sub> ) <sub>2</sub> CH <sub>2</sub> NH <sub>2</sub>	37	Neu5Gca6Galβ4GlcNacβ2Mana3(Neu5Gca6Galβ4GlcNacβ2Mana6)Manβ4GlcNacβ4GlcNacitol-AEAB	3	
28	Neu5Gca6GalβO(CH <sub>2</sub> ) <sub>2</sub> CH <sub>2</sub> NH <sub>2</sub>	69	Neu5Gca6Galβ3GlcNacβ3Galβ4Glcitol-AEAB	3	
31	Neu5.9Ac <sub>2</sub> α6GalβO(CH <sub>2</sub> ) <sub>2</sub> CH <sub>2</sub> NH <sub>2</sub>	5	Neu5.9Ac <sub>2</sub> α6Galβ4GlcNacβ3Galβ4Glcitol-AEAB	3	
31	Neu5.9Ac <sub>2</sub> α6GalβO(CH <sub>2</sub> ) <sub>2</sub> CH <sub>2</sub> NH <sub>2</sub>	38	Neu5.9Ac <sub>2</sub> α6Galβ4GlcNacβ2Mana3(Neu5.9Ac <sub>2</sub> α6Galβ4GlcNacβ2Mana6)Manβ4GlcNacβ4GlcNacitol-AEAB	3	
32	Neu5Gc9Aca6GalβO(CH <sub>2</sub> ) <sub>2</sub> CH <sub>2</sub> NH <sub>2</sub>	6	Neu5Gc9Aca6Galβ4GlcNacβ3Galβ4Glcitol-AEAB	3	
32	Neu5Gc9Aca6GalβO(CH <sub>2</sub> ) <sub>2</sub> CH <sub>2</sub> NH <sub>2</sub>	39	Neu5Gc9Aca6Galβ4GlcNacβ2Mana3(Neu5Gc9Aca6Galβ4GlcNacβ2Mana6)Manβ4GlcNacβ4GlcNacitol-AEAB	3	
11	Neu5Aca3Galβ4GlcNacβO(CH <sub>2</sub> ) <sub>2</sub> CH <sub>2</sub> NH <sub>2</sub>	48	Neu5Aca3Galβ4GlcNacβ2Mana3(Neu5Aca3Galβ4GlcNacβ2Mana6)Manβ4GlcNacβ4GlcNacitol-AEAB	3	
12	Neu5Gca3Galβ4GlcNacβO(CH <sub>2</sub> ) <sub>2</sub> CH <sub>2</sub> NH <sub>2</sub>	50	Neu5Gca3Galβ4GlcNacβ2Mana3(Neu5Gca3Galβ4GlcNacβ2Mana6)Manβ4GlcNacβ4GlcNacitol-AEAB	3	
1	Neu5.9Ac <sub>2</sub> α3Galβ4GlcNacβO(CH <sub>2</sub> ) <sub>2</sub> CH <sub>2</sub> NH <sub>2</sub>	52	* Neu5.9Ac <sub>2</sub> α3Galβ4GlcNacβ2Mana3(Galβ4GlcNacβ2Mana6)Manβ4GlcNacβ4GlcNacitol-AEAB	3	
2	Neu5Gc9Aca3Galβ4GlcNacβO(CH <sub>2</sub> ) <sub>2</sub> CH <sub>2</sub> NH <sub>2</sub>	53	Neu5Gc9Aca3Galβ4GlcNacβ2Mana3(Neu5Gc9Aca3Galβ4GlcNacβ2Mana6)Manβ4GlcNacβ4GlcNacitol-AEAB	3	
17	Neu5Aca6Galβ4GlcNacβO(CH <sub>2</sub> ) <sub>2</sub> CH <sub>2</sub> NH <sub>2</sub>	35	Neu5Aca6Galβ4GlcNacβ2Mana3(Neu5Aca6Galβ4GlcNacβ2Mana6)Manβ4GlcNacβ4GlcNacitol-AEAB	3	
18	Neu5Gca6Galβ4GlcNacβO(CH <sub>2</sub> ) <sub>2</sub> CH <sub>2</sub> NH <sub>2</sub>	37	Neu5Gca6Galβ4GlcNacβ2Mana3(Neu5Gca6Galβ4GlcNacβ2Mana6)Manβ4GlcNacβ4GlcNacitol-AEAB	3	
3	Neu5.9Ac <sub>2</sub> α6Galβ4GlcNacβO(CH <sub>2</sub> ) <sub>2</sub> CH <sub>2</sub> NH <sub>2</sub>	38	Neu5.9Ac <sub>2</sub> α6Galβ4GlcNacβ2Mana3(Neu5.9Ac <sub>2</sub> α6Galβ4GlcNacβ2Mana6)Manβ4GlcNacβ4GlcNacitol-AEAB	3	
4	Neu5Gc9Aca6Galβ4GlcNacβO(CH <sub>2</sub> ) <sub>2</sub> CH <sub>2</sub> NH <sub>2</sub>	39	Neu5Gc9Aca6Galβ4GlcNacβ2Mana3(Neu5Gc9Aca6Galβ4GlcNacβ2Mana6)Manβ4GlcNacβ4GlcNacitol-AEAB	3	
45	Galβ4GlcNacβO(CH <sub>2</sub> ) <sub>2</sub> CH <sub>2</sub> NH <sub>2</sub>	78	Galβ4GlcNacβ3Galβ4Glcitol-AEAB	2	